J. Phycol. **42,** 170–193 (2005)

DOI: 10.1111/j.1529-8817.2006.00172.x

ON THE IDENTITY OF *KARLODINIUM VENEFICUM* AND DESCRIPTION OF *KARLODINIUM ARMIGER* SP. NOV. (DINOPHYCEAE), BASED ON LIGHT AND ELECTRON MICROSCOPY, NUCLEAR-ENCODED LSU rDNA, AND PIGMENT COMPOSITION[1]

Trine Bergholtz, Niels Daugbjerg, Øjvind Moestrup[2]

Department of Phycology, Biological Institute, University of Copenhagen, Øster Farimagsgade 2D, DK-1353 Copenhagen K, Denmark

and

Margarita Fernández-Tejedor

Centro d'Aquicultura–IRTA, Carretera del Pobleno s/n, Sant Carles de la Rapita 43540, Spain

An undescribed species of the dinoflagellate genus *Karlodinium* J. Larsen (viz. *K. armiger* sp. nov.) is described from Alfacs Bay (Spain), using light and electron microscopy, pigment composition, and partial large subunit (LSU) rDNA sequence. The new species differs from the type species of *Karlodinium* (*K. micrum* (Leadbeater et Dodge) J. Larsen) by lacking rows of amphiesmal plugs, a feature presently considered to be a characteristic of *Karlodinium*. In *K. armiger*, an outer membrane is underlain by a complex system of cisternae and vacuoles. The pigment profile of *K. armiger* revealed the presence of chlorophylls *a* and *c*, with fucoxanthin as the major carotenoid. Phylogenetic analysis confirmed *K. armiger* to be related to other species of *Karlodinium*; thus forming a monophyletic genus, which, in the LSU tree, occupies a sister group position to *Takayama* de Salas, Bolch, Botes et Hallegraeff. The culture used by Ballantine to describe *Gymnodinium veneficum* Ballantine (Plymouth 103) was examined by light and electron microscopy and by partial LSU rDNA. Ultrastructurally, it proved identical to *K. micrum* (cultures Plymouth 207 and K. Tangen KT-77D, the latter also known as K-0522), and in LSU sequence, differed in only 0.3% of 1438 bp. We consider the two taxa to belong to the same species. This necessitates a change of name for the most widely found species, *K. micrum*, to *K. veneficum*. The three genera *Karlodinium*, *Takayama*, and *Karenia* constitute a separate evolutionary lineage, for which the new family Kareniaceae fam. nov. is suggested.

Key index words: ***Karlodinium armiger*; *Karlodinium micrum*; *Karlodinium veneficum*; *Karlodinium vitiligo*; LSU rDNA phylogeny; ultrastructure**

Abbreviations: **LM, light microscopy; ML, maximum likelihood; MP, maximum parsimony; NJ, neighbor-joining; TBR, branch-swapping algorithm**

Until recently, the genus *Gymnodinium* F. Stein comprised a diverse assemblage of naked (unarmored) dinoflagellates. A comparative study using morphological features, particularly the outline of the apical groove, in addition to the composition of photosynthetic pigments, and nuclear-encoded large subunit (LSU) rDNA sequences, clearly showed that *Gymnodinium* was polyphyletic (Daugbjerg et al. 2000). Two fucoxanthin-containing genera, *Karenia* Gert Hansen et Moestrup (with three species), and *Karlodinium* J. Larsen (also with three species) were proposed, and the description of *Gymnodinium* was emended (Daugbjerg et al. 2000). In less than 5 years, the known diversity of *Karenia* has escalated, and 10 species have now been described, while the number of described *Karlodinium* species has grown to four. Recently, a third fucoxanthin-containing genus, *Takayama* de Salas, Bolch, Botes et Hallegraeff, was shown to be related to *Karenia* and *Karlodinium* (de Salas et al. 2003). Hence, a distinct evolutionary lineage with three genera of naked dinoflagellates has now been established, well supported by bootstrap values (de Salas et al. 2003). This lineage shares a single synapomorphic character relating to the chloroplasts (symbiont): fucoxanthin and its derivatives are the major accessory pigments. Unfortunately, the nearest sister group to this lineage has not been determined by gene sequences (Daugbjerg et al. 2000, de Salas et al. 2003). Several species in the lineage are known to be ichthyotoxic (e.g., *Karenia brevis* (Davis) Gert Hansen et Moestrup, *K. mikimotoi* (Miyaki et Kominami ex Oda) Gert Han-

[1]Received 15 March 2005. Accepted 26 October 2005.
[2]Author for correspondence: e-mail moestrup@bi.ku.dk.

sen et Moestrup, *K. brevisulcata* (Chang) Gert Hansen et Moestrup, *K. bicuneiformis* Bootes, Sym et Pitcher, *K. papilionacea* Haywood et Steidinger, *K. selliformis* Haywood, Steidinger et McKenzie, *Karenia umbella* de Salas, Bolch et Hallegraeff, *Takayama cladochroma* (J. Larsen), de Salas, Bolch et Hallegraeff, and *Karlodinium micrum* (Leadbeater et Dodge) J. Larsen) and thus, pose a threat to the marine environment, in particular to cultured fish (Abbott and Ballantine 1957, Fraga and Moestrup 2004). Identification of species belonging to *Karenia*, *Karlodinium*, and *Takayama* often requires live samples, and important species characteristics are cell shape, outline of the sulcus and cingulum on the ventral side of the cell, and the arrangement of chloroplasts. Some of these features are often ambiguous in fixed material; indeed, material prepared for SEM may not be sufficient for identification of species assigned to the genus *Takayama* (de Salas et al. 2003).

One of the morphological characters separating *Karlodinium* and *Karenia* is the presence of a ventral pore and a unique type of amphiesma with plugs in *Karlodinium*. Daugbjerg et al. (2000) discussed including *Gyrodinium corsicum* Paulmier, Berland, Billard et Nezan in *Karlodinium* (Daugbjerg et al. 2000), but information on the amphiesma of this species was not available. Winter blooms referred to *G. corsicum* have occurred annually in Alfacs Bay (Spain) since 1994 (Delgado 1998), associated with killing of *Sparus aurata* Linnaeus (gilthead seabream) in aquaculture ponds, and *Mytilus galloprovincialis* Lam in raft cultures, in addition to causing mortality of wild fauna. The chemical identity of the toxic compound has not been established, but *G. corsicum* has also been reported to have a noxious effect on the copepod *Acartia grani* Sars (Delgado and Alcaraz 1999).

To examine the identity and taxonomy of the ichthyotoxic *G. corsicum*, we studied a clonal culture from Alfacs Bay by light and electron microscopy, and we also examined its pigment composition and partial LSU rDNA sequence. However, the isolate proved to differ morphologically from *G. corsicum* as described by Paulmier et al. (1995), and we consider it to belong to a new species of *Karlodinium*, *K. armiger* sp. nov. We also examined the original clonal culture of *Karlodinium veneficum* (Ballantine) J. Larsen (Plymouth collection no. 103), which has been in culture in Plymouth since 1950. Although the fixation of the culture for TEM was not optimal, we could find no significant difference in ultrastructure between this strain and *K. micrum* (Tangen strain, the original strain has been lost), and the LSU rDNA sequences diverged by only 0.3%, based on 1438 bp of LSU rDNA. We therefore conclude that the two taxa are conspecific. As *G. veneficum micrum* Ballantine is the oldest name, this has implications for the naming of isolates presently known as *K. micrum*. We emend the diagnosis of the genus *Karlodinium* following the new observations, and a new family, Kareniaceae, is suggested to comprise *Karenia*, *Karlodinium*, and *Takayama*.

MATERIALS AND METHODS

Culture conditions. The Spanish isolate was established into clonal culture by M. Fernández-Tejedor. It originated from a water sample collected at Alfacs Bay, Ebro Delta, NW Mediterranean (Fig. 1), and it is now deposited in the Scandinavian Culture Collection of Algae and Protozoa as K-0668. It is maintained at 15 and 20° C in TL-medium (see http://www.sccap.bot.ku.dk/media/) at a salinity of 30 psu and a 12:12 LD regime. Illumination is *approximately* 28 µmol · photons · $m^{-2} \cdot s^{-1}$. Clonal cultures of *K. micrum* (Leadbeater et Dodge) J. Larsen (K-0522, originally isolated by K. Tangen as KT-77D using the name *Gymnodinium galatheanum* Braarud) and *G. veneficum* Ballantine (Plymouth collection no. 103), were also examined. The former was grown under the same conditions as the Spanish culture. Plymouth 103 was examined in Plymouth, because all attempts of transport to Copenhagen failed. Cultures of *Karlodinium* used in this study are listed in Table 1.

Light microscopy. Live cells of K-0668 and K-0522 were observed using an Olympus Provis AX70 microscope equipped with Nomarski interference contrast optics (Olympus, Tokyo, Japan) and micrographs were taken with a Zeiss Axio Cam digital camera (Zeiss, Oberkochen, Germany). Chloroplast number and arrangement were visualized by epifluorescence microscopy.

Cell measurements. Live cells of K-0668 and K-0522, in the exponential phase, were digitally recorded using an Olympus BX60 microscope and a Sony 3CCD color video camera (Tokyo, Japan). Video sequences were frame grabbed and individual frames were exported in JPEG format. The length

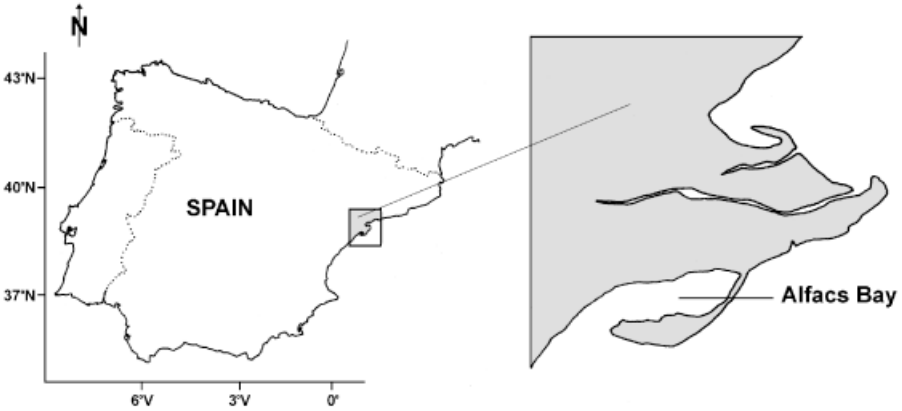

FIG. 1. Map of Spain (left) showing location of Alfacs Bay where *Karlodinium armiger* sp. nov. was sampled.

TABLE 1. Species of *Karlodinium* used for studies on nuclear-encoded large subunit (LSU) rDNA.

Species	Locality	Year of isolation	Isolated by	Strain number	GenBank accession number
Karlodinium armiger	Alfacs Bay, Spain	2000	M. Fernández-Tejedor	K-0668	DQ114467
Karlodinium australe	Tasmania, Australia	2002	M. de Salas	KDAGT03	DQ151559
Karlodinium veneficum	Oslofjord, Norway	1977	K. Tangen	K-0522	AF200675
Karlodinium veneficum	Devonport, UK	1950	M. Parke	Plymouth 103	DQ114466

and width of randomly selected cells ($n = 51$) were measured on a PC, using the UTHSCSA Imagetool program (developed at University of Texas Health Science Center at San Antonio, Texas).

SEM. Cultures of K-0668 and K-0522 were fixed for 2 h in six volumes of 2% OsO_4 diluted in seawater (30 psu) and one volume saturated aqueous $HgCl_2$ solution (SEM of Plymouth 103, though attempted, was not satisfactory). The cells were then filtered onto a Millipore filter (8 μm) and washed in distilled water for 2 h. The sample was subsequently dehydrated in an ethanol series (30, 50, 70, 96, and 99.9%), 20 min in each change; followed by two rinses in 99.9%, 30 min in each change. The sample was critical-point-dried in liquid CO_2 in a Baltec CPD30 critical-point-drying apparatus (Bal-Tec, Balzars Liechtenstein), and the filter was subsequently glued to SEM-stubs with double-adhesive carbon disks. Stub and filter was sputter-coated with platinum and examined in a JSM-6335F scanning electron microscope (Jeol, Tokyo, Japan) at the Zoological Museum, University of Copenhagen.

TEM. A culture of K-0668 was fixed in 2% glutaraldehyde in 0.1 M NaCacodylate-buffer containing 0.2 M sucrose. After 75 min, cells were pelleted by centrifugation and washed in three steps of buffer solution containing decreasing concentrations of sucrose. It was post-fixed for 1 h in 1% OsO_4 made up in medium, washed quickly in medium and dehydrated in an ethanol series (5, 30, 50, 70, and 96%, followed by two changes of 99.9%). Dehydration was completed in two changes of propylene oxide, 10 min in each change. The material was embedded in Spurr's resin and sectioned on an LKB 8800 microtome (LKB, Bromma, Sweden) using a diamond knife. The sections were mounted on slot grids, stained with uranyl acetate and lead citrate, and examined in a JEOL-1010 electron microscope (Jeol).

A culture of Plymouth 103 was collected at the Marine Biological Association of the UK, Plymouth, quickly transported to the Electron Microscopy Centre at the University of Plymouth, and processed there. The sample was fixed for 3 h at room temperature in an equal volume of 4% glutaraldehyde in growth medium or in 0.1 M cacodylate buffer containing 0.25 M sucrose, centrifuged into a pellet, and rinsed in three changes of medium over $1\frac{1}{2}$ h before post-osmication in 2% OsO_4 in distilled water for 1 h at 4° C. Dehydration and embedding in Spurr's embedding medium were as described above.

Pigment analysis. An exponentially growing culture of *K. armiger* (40 mL) was gently filtered onto a 25 mm Advantec GF 75 glass fiber filter (Toyo Roshi Kaisha, Tokyo Japan) and immediately stored in the freezer at −80° C. The filters were subsequently transferred to 2.5 mL methanol, sonicated for 30 s and filtered (0.2 μm). The extract (1 mL) was mixed with 250 μL water just prior to pigment analysis. The high-performance liquid chromatography (HPLC) analyses were performed on a Shimadzu LC 10A system (Shimadzu, Kyoto Japan) with a Supercosil C18 column (250 mm × 4.6 mm, 5 μm) located at the National Environmental Research Institute, Denmark, using a slight modification of the method described in Schlüter and Havskum (1997). Pigments were identified by retention times and absorption spectra identical to those of authentic standards, and quantified against standards purchased from the International Agency for C14 Determination (Hørsholm, Denmark).

DNA extraction and amplification of LSU rDNA. Clonal cultures (20 mL) of *K. armiger*, *K. selliformis*, and *K. veneficum* were harvested by centrifugation (1500 rpm, 1125 ***g***) for 10 min at room temperature and transferred to a 1.5 mL Eppendorf tube. The pellets were kept frozen at −20° C until extraction of DNA (at least 1 day). Total genomic DNA was extracted as described in Daugbjerg et al. (1994) and used as a template to amplify approximately 1400 bp of the LSU rDNA gene using terminal primers D1R and 28-1483R. Conditions for PCR amplification and thermal cycling were followed as outlined in Hansen et al. (2000). The PCR product was purified using the QIAquick PCR purification Kit (Qiagen Chatsworth, CA, USA), and nucleotide sequences were determined using the Dye Terminator Cycle Sequencing Ready Reaction Kit (Perkin Elmer, Foster City, CA, USA). The cycle sequencing reactions were run on an ABI PRISM 377 DNA Sequencer (Perkin Elmer), according to the recommendations of the manufacturer.

Alignment and phylogenetic analyses. The LSU rDNA gene sequences determined from the three species of *Karlodinum* were added to a data matrix comprising two other sequences of *Karlodinium* (*K. australe* and *K. micrum*), seven species of *Karenia* (eight sequences), and three species of *Takayama* (five sequences). These species were recently shown to form a well-supported monophyletic group (de Salas et al. 2003), and because our specific interest was to examine the phylogeny of *Karlodinum*, we used four species of *Gymnodinium* as an outgroup. Information from the secondary structure of LSU rRNA was included as suggested by de Rijk et al. (2000), and a total of 1438 bp were analyzed with maximum likelihood (ML), maximum parsimony (MP), and Neighbor-joining (NJ) methods using PAUP* (ver. 4b10, Swofford 2003). A 71 bp long fragment was excluded because of ambiguous alignment. This fragment was part of the highly variable domain D2. To obtain the best model for ML analysis, we applied Modeltest (ver. 3.06, Posada and Crandall 1998). Among the 56 models tested, the TrN + I + G model (Tamura and Nei 1993) was suggested as the best fit for the data matrix. Among sites, rate heterogeneity (α) was 0.6551, an estimated proportion of invariable sites ($I = 0.4685$) and two substitution rate categories (A–G = 2.181 and C–T = 6.4388). Base frequencies were set at A = 0.2621, C = 0.1866, G = 0.2829, and T = 0.2684. A total of 100 random additions were performed in ML. In parsimony analysis, 10,000 random additions were performed using the heuristic search option and a branch-swapping algorithm (TBR). All characters were unordered, weighted equally and gaps were treated as missing data. For NJ analysis, we used the model suggested by Modeltest to compute dissimilarity values, and these were used to construct a tree. To examine the robustness of the tree topology, bootstrap analyses were conducted with 100 replications in ML, 10,000 in MP, and 1000 in NJ.

RESULTS

Karlodinium armiger Bergholtz, Daugbjerg et Moestrup sp. nov.

Cellulae ovales, 12–22 μm longae et 8–18 μm latae, epiconus conicus, hypoconus rotundatus, hypoconus paulo major quam epiconus. Cellulae non complanatae. Cingulum latitudine duorum cingulorum, circa tertiis longitudinis cellulae remotum. Pars anterior cinguli acute ab epicono per vittam delineata; pars posterior levis in hypoconum extensa. Sulcus in epiconum extensus. Porus elongatus in latere sinistro epiconi, a base apicalis canaliculi. Decem aut plures pallidovirides chloroplasti peripheriam cellulae circumeuntes, quorum quisque pyrenoidem internam lenticularem lamina tenui limitatam habet. Pigmentum chloroplasti principalis fucoxanthinum. Nucleus dorsalis in parte sinistra hypoconi, sed in epiconum extensus.

Cells oval, 12–22 μm long and 8–18 μm wide, epicone conical, hypocone rounded, hypocone slightly larger than epicone. Cells not flattened. Cingulum displaced approximately two cingulum widths, approximately one-third the cell length. Anterior side of cingulum sharply delineated from the epicone by a list, the posterior side extending smoothly into the hypocone. The sulcus extends onto the epicone. Elongate ventral pore present on the left side of the epicone, to the left of the apical groove. Ten or more pale-green chloroplasts located along the cell periphery, each with an internal lenticular pyrenoid bounded by a thin plate-like structure. Main chloroplast pigment fucoxanthin. Nucleus dorsal, in the left side of the hypocone but extending into the epicone.

Holotype. A fixed and embedded sample of culture K-0668 has been deposited at the Botanical Museum, Copenhagen University (C) as No. A-2381, and serves as type material. A subculture has been deposited in the Scandinavian Culture Centre for Algae and Protozoa. Figures 2–11 all illustrate this material.

Type locality: Alfacs Bay, Ebro Delta, NW Mediterranean (Fig. 1).

Etymology: Named after the many trichocysts in the peripheral part of the cell.

Distribution: Presently known only from the type locality.

Light microscopy. K. armiger has an average length of 17.4 ± 2.4 μm (range 12.3–22.4 μm) and an average width of 13.1 ± 1.8 μm (range 8.3–17.8 μm) ($n = 50$). The data are presented in Table 2, for comparison with *K. micrum*, *K. veneficum*, *K. vitiligo* (Ballantine) J. Larsen, *G. corsicum*, and *Gyrodinium estuariale* Hulburt. Cells are slightly asymmetrical and oval (Fig. 2A), the hypocone being slightly larger than the epicone. The epicone is conical while the hypocone is rounded and incised, the right side being longer than the left side (Fig. 2A). The cingulum is left-handed and deeply excavated, and displaced about two cingulum widths. The displacement is approximately one-third the body length (Fig. 2A, C, D). The sulcus continues as an extension onto the epicone just above the epicone–cingulum border. This extension is readily visible and points upward to the right (Fig. 2C). The sulcus is wide in the hypocone, but becomes markedly narrower in the intercingular region (Fig. 2C). The deep apical groove can sometimes be seen as a straight line when focusing on the cell surface (Fig. 2D). Several (>10) pale yellow-green chloroplasts are located along the periphery of both the epi- and hypocone (Fig. 2A, E). The large oval- or kidney-shaped nucleus is usually visible on the left side of the hypocone (Fig. 2B). Diagrammatic representations of the cell are shown in Fig. 3, in ventral and dorsal view, respectively. Planozygotes with two parallel longitudinal flagella (von Stosch 1973) were identified in light microscopy (LM), SEM, and TEM, but the complete life cycle was not determined. Fusing cells were seen, either with fusing parallel epicones or with the apex perpendicular to the mid-central sulcus (Fig. 4). Cysts were never observed.

SEM. The apical groove is distinct, and extends just above the sulcal extension on the ventral side of the cell (Fig. 2F). It continues in a slight curve, bypasses the apex, and extends to about one-fourth the length of the epicone on the dorsal side of the cell (Fig. 2G). The groove is deeply incised and about 0.5 μm wide proximally on the ventral side, while the dorsal termination is markedly narrower (Fig. 2F–H). A ventral pore is present to the left of the apical groove. It is elongate and about 1 μm long (Fig. 2F). The ventral ridge between the two flagellar pores is distinctly thickened. The angle between the sulcal extension and the ventral ridge is at least 90° and appears as a soft curve in ventral view. From other angles, the same area seems rather pointed (Fig. 2F, H). The lower part of the ventral ridge, together with the right part of the lower epicone, is very pointed. This extension hides the basal part of the transverse flagellum and the proximal part of the cingulum canal (Fig. 2I). In SEM, membranous material is often seen to cover the cell surface. In some of our fixations, the cells retained the outermost membrane and the amphiesma appeared as a set of polygonal vesicles (e.g., the hypocone in Fig. 2F). In other fixations, both the outermost and the superficial vesicle membrane had disappeared and the vesicles were clearer (Fig. 2I). The membrane present, possibly the inner vesicle membrane, was granulated and showed some larger, rounded structures (Fig. 2J), randomly placed on the cell surface. In many cases, cells had a double set of flagella, and such cells (planozygotes) were, on the whole, better fixed. The transverse flagella were seen to carry a row of fine hairs, while no appendages were visible on the longitudinal flagella (Fig. 2F, G).

TEM. General morphology: Figure 5A, B shows the main organelles in the cell: the chloroplasts scattered in the cell periphery, the nucleus along the dorsal side of the cell (Fig. 5B)—and although in LM, it is seen to be present in the posterior part of the cell, it does in fact extend into the epicone (Fig. 5A, B). Figure 5A, B also shows numerous vacuoles, including

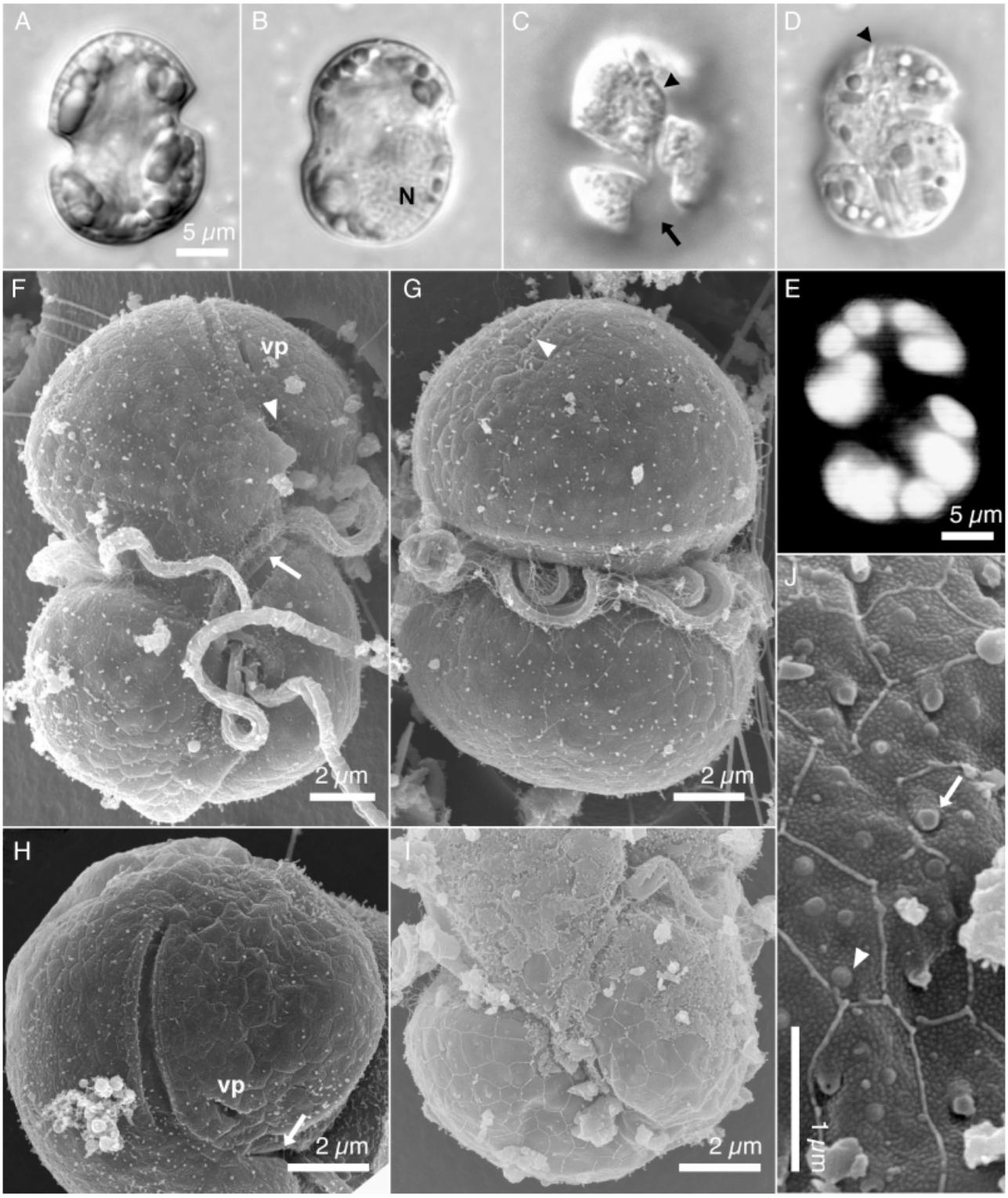

FIG. 2. Light micrographs, epifluorescence and scanning electron micrographs of *Karlodinium armiger* sp. nov. (A) Central focus showing numerous peripheral chloroplasts. (B) Ventral view (deep focus) showing the nucleus (N) on the viewer's right. (C) Ventral view of cell in surface focus, showing sulcal intrusion into epicone (arrowhead) and the wide sulcus (arrow). (D). Ventral view showing the apical groove (arrowhead). (E) Central focus showing numerous peripheral chloroplasts in epifluorescence. (F) Ventral view of planozygote, showing the sulcal intrusion onto the epicone (arrowhead) and a distinct ventral ridge (arrow). The ventral pore (vp) is also visible. (G) Dorsal view of cell showing two transverse flagella and the termination of the apical groove on the dorsal side (arrowhead). (H) Cell showing apical groove, vp, and sulcal intrusion onto the epicone (arrow). (I) Ventral view of hypocone, showing amphiesma vesicles. The outer membrane has disappeared. (J) Magnification of the amphiesma vesicles, showing granulated structure of the vesicles, and numerous trichocysts. Some trichocysts are intact (arrowhead) while others have discharged (arrow).

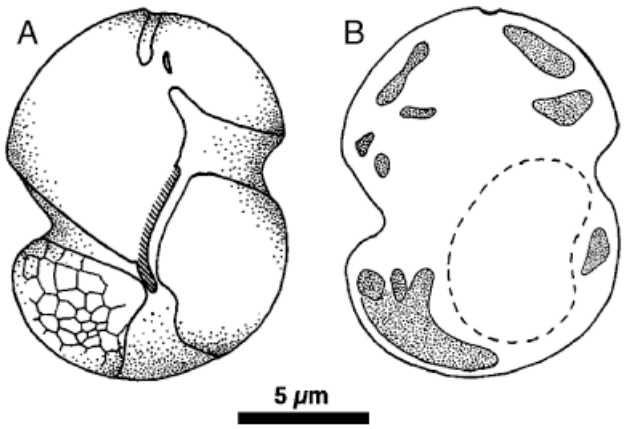

FIG. 3. Drawings of *Karlodinium armiger* sp. nov. (A) Ventral view. (B) Position of nucleus (bounded by a dashed line) and profiles of chloroplasts (shaded).

a possible food vacuole located posteriorly in Figure 5B, and the prominent ventral ridge lined by the two flagellar canals (Fig. 5B, right).

The cell covering, apical groove, the cingulum list. The cell was covered with a continuous layer of semi-opaque material located immediately beneath the outer membrane (w in Fig. 5E). It was seen in all cells studied, vegetative cells as well as planozygotes. In the flagellar area, however, amphiesmal vesicles (Fig. 7A) were located above the semi-opaque material. Based on the observations from SEM, we believe that the amphiesma vesicles may have disappeared on the rest of the cell during fixation. The origin of the continuous layer of wall material has not been ascertained.

The apical groove is very distinct and in Figure 5C, D, is approximately 0.5 μm wide and approximately 0.30 μm deep. The two rims bordering the groove are different such as: on one side, the rim is supported by a group of three to four microtubules close together, overlaying an indistinct vesicle, an opaque rod and two additional, but somewhat separated microtubules; the other rim is supported by a vacuole containing a narrow plate of opaque material, and two microtubules are located a short distance away.

The two rims of the cingulum are also different. The anterior rim projects as a list, supported by microtubules (Fig. 5E), while the posterior rim curves more or less evenly into the hypocone. Because the difference between the two sides of the cingulum is pronounced, the epi- and hypocone are readily distinguished in the thin sections (Fig. 5A, B).

Chloroplasts: All chloroplasts possess central lenticular pyrenoids, the matrix of which is penetrated by a few tubules (three in Fig. 6A). The pyrenoid matrix is bounded by a very thin opaque plate, which is sometimes seen to extend as a distinct beak (Fig. 6B).

The peripheral part of the cytoplasm, trichocysts: The detailed construction of the amphiesma was difficult to understand, but once a series of tangential sections through the cell periphery had been obtained, its structure was clarified. Two sections from the series are reproduced as Figure 7B, C. In contrast to *K. micrum*, *K. armiger* lacks plugs. Instead, the outer membrane is underlain by a complex system of cisternae and vacuoles. The vacuoles contain electron-

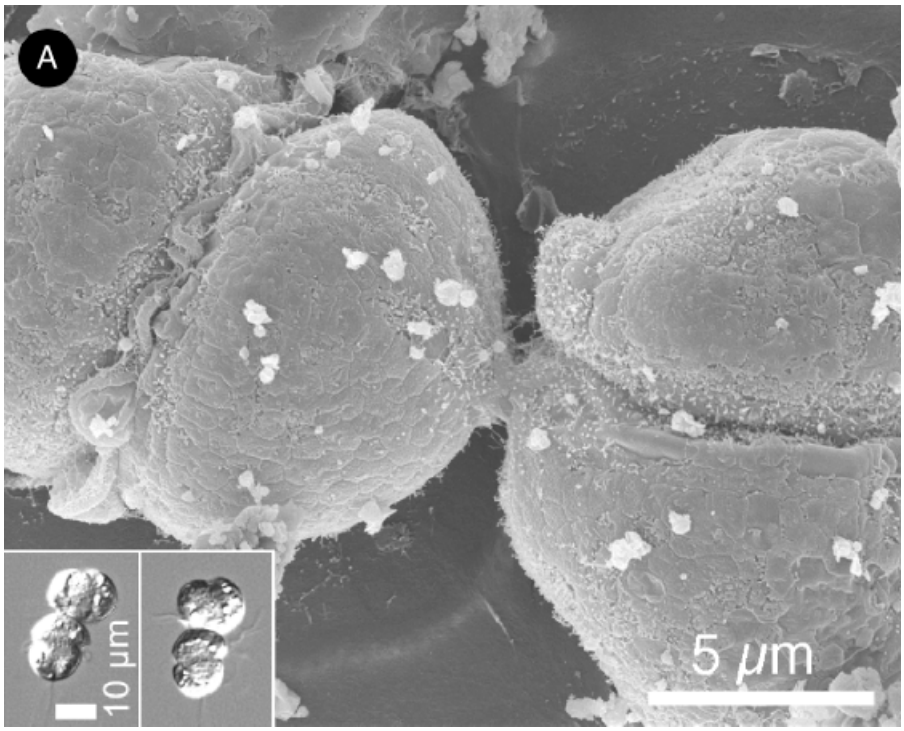

FIG. 4. *Karlodinium armiger* sp. nov. (A) Scanning electron micrograph showing what is believed to be sexual fusion (note the connection between the apical area of the left gamete and the mid-ventral area of the right gamete. Insets illustrate apparent cell fusion as seen in the light microscope.

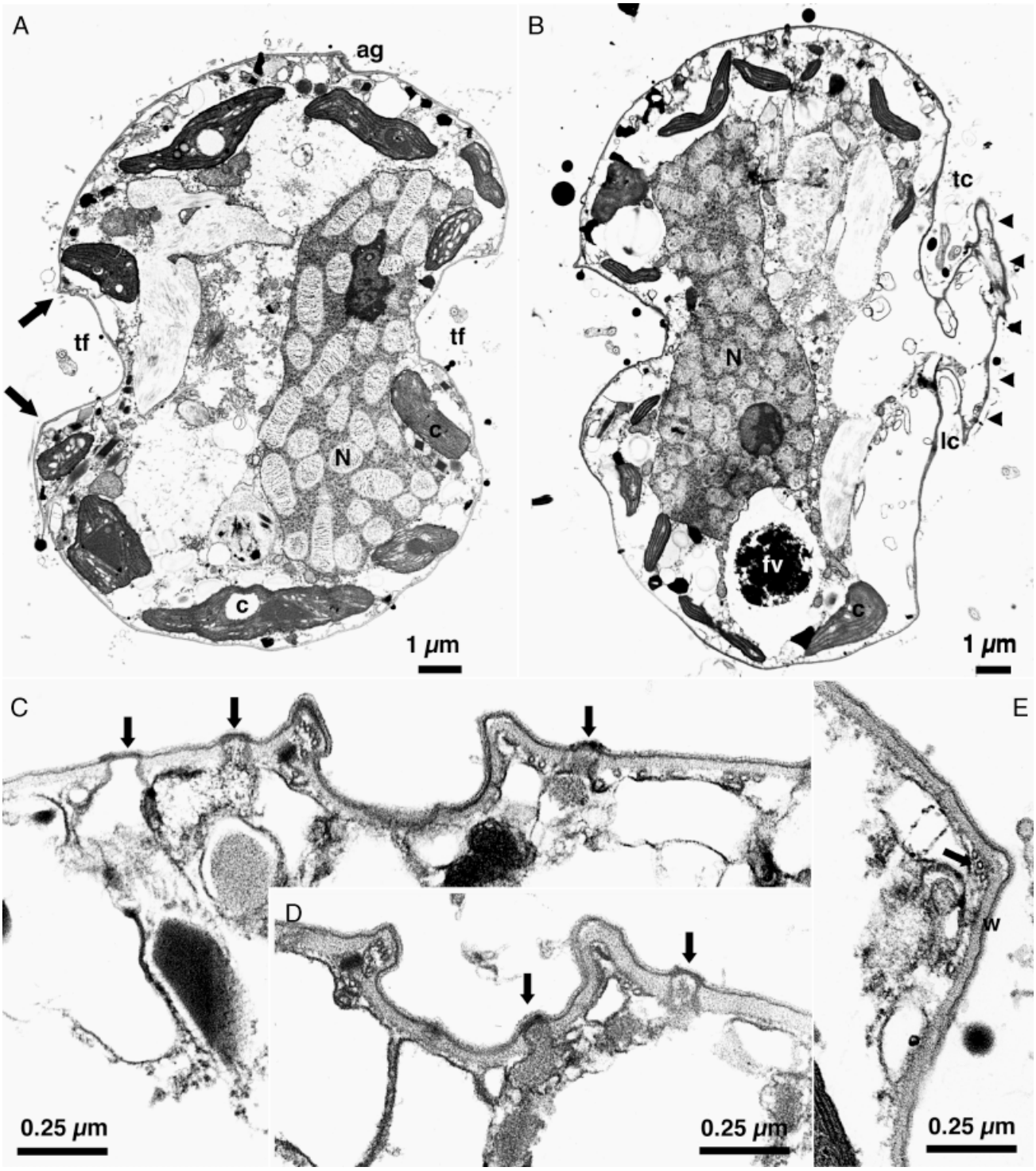

FIG. 5. *Karlodinium armiger* sp. nov. (A, B) Longitudinal sections at nearly right angles to each other (A, ventral view; B, right side view). In (A), the cell has been sectioned in a lateral plane, showing the nucleus (N) in the left hand side of the cell (viewer's right). Chloroplasts (c) are scattered in the cell periphery, and in (B), a food vacuole-like inclusion (fv) is present near the antapical end. The anterior border of the cingulum is list-like while the posterior border is more or less smooth (arrows). The transverse flagellum (tf) is visible in the cingulum. The apical groove (ag) has been sectioned obliquely in (A). The cell in (B) illustrates the ventral "flap" with the ventral ridge (arrowheads), the dorsally located nucleus (N), and the canal of the longitudinal (lc) and transverse flagellum (tc). (C, D) Details of the apical groove, showing the different construction of the two sides (see text for details). (E) The anterior list of the cingulum is supported by microtubules (arrow). W, semi-opaque "wall" material.

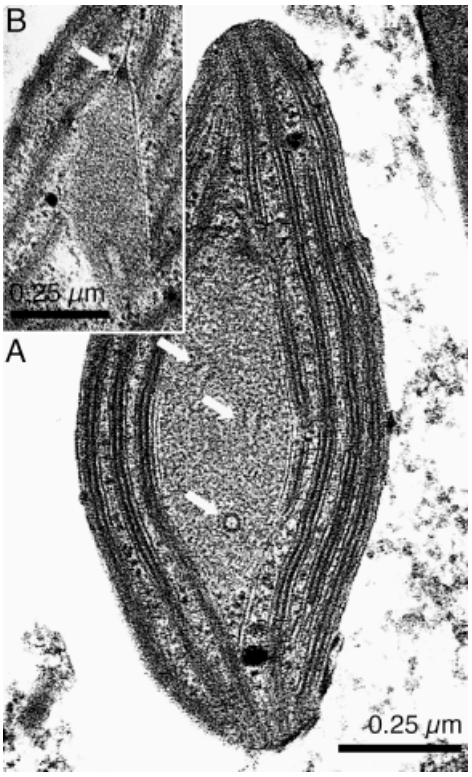

FIG. 6. Chloroplasts of *Karlodinium armiger* sp. nov. (A) Whole chloroplast showing internal pyrenoid surrounded by thin plate-like structure, and profiles of three tubular structures within the pyrenoid matrix (arrows). (B) The plate-like structure surrounding the pyrenoid is sometimes seen to extend into a wing (arrow).

opaque material, and fixed cells had often discharged their contents to the exterior. They are seen as opaque spheres surrounding the cell in Figure 7B, C. Vacuoles still containing their opaque contents are present in Figure 7B, C, E. The second component of the amphiesma is a system of elongated cisternae in which each cisterna contains a trichocyst. The trichocyst is divided into two parts as in other dinoflagellates, a long thinner neck region measuring approximately 0.04–0.05 μm in width, and the thicker (approximately 0.2 μm at its widest) proximal part (Figs. 7D, E and 8A, C). The distal part of each trichocyst-containing cisterna is closely appressed to the outer cell membrane, and the contact point is somewhat thickened to form a lid-like structure (Fig. 7B, E). Discharging trichocysts are visible in Figures 7E and 8C. Figure 7F is a transverse section through the amphiesma region, showing the square or rhomboid neck region of three trichocysts, compare with the trichocyst pair in Figure 8C. There seems to be a particularly high concentration of the trichocysts on the epicone, and thus Figure 5C shows three trichocysts, and in Figure 5D, a trichocyst even seems to be opening into the apical groove. The cell periphery is further supported by groups of microtubules beneath the semi-opaque wall material (Fig. 5C).

The internal parts of the flagellar apparatus, the peduncle. These structures will only be discussed in a general way here. The two flagella are almost opposite (Fig. 8C), or more precisely inserted at an angle of approximately 150–155° to each other. Each flagellum leaves the cell through a separate canal (lc and tc in Fig. 8A, C, which are from the same series of sections). Figure 8A, C also shows part of the collars that surround the flagellar canals (also visible in Fig. 7A). Parts of three flagellar roots are visible in Figure 8A–C. Root r_1 passes from the longitudinal flagellum base, in a posterior direction along the sulcus (Fig. 8A–C). Root r_3 extends from the transverse flagellum base to the canal of this flagellum, nucleating a group of microtubules, visible in Figure 8A, C (known as the root extension). Root r_4 is visible as an opaque area next to the transverse flagellum base, shown in Fig. 8A–C. This root is exceptionally well developed in *K. armiger* (Fig. 11B): the transverse fiber that extends along the pusule system in the figure is the cross-banded component of r_4. Figure 8B also illustrates the fiber that interconnects r_1 and r_4 (the striated root connective, src). The peduncle system comprises a band of microtubules (not shown) and a group of electron-opaque vesicles, visible in Figure 8A. We plan to examine the structure of the peduncle and the internal part of the flagellar apparatus in more detail.

The transverse flagellum: The transverse flagellum (Fig. 9A–F) is complex and carries a unilateral wing supported distally by a fibrous rod (e.g., Fig. 9A, E, F), which is occasionally seen to be cross-banded (Fig. 9C). However, the wing also contains another, more opaque structure (Fig. 9A–E). This is not a continuous structure, and Figure 9E is from a series of four sections in which the opaque strand was visible only in the two middle sections. Whether there are more strands present in the flagellum is not known, but it is possible that several of these strands are present, located in the curvatures of the flagellum (Fig. 9E), near the axoneme (Fig. 9D). The position of the strand indicates a function in bending of the flagellum. Externally the axonemal part of the flagellum carries hair-like appendages. The most conspicuous is a series of approximately 0.2 μm long, thick hooks, separated from each other by a distance of ~ 0.10 μm (Fig. 9A, B). The hooks insert on the axoneme at right angles to the plane of the wing-like part of the flagellum and are probably attached through the flagellar membrane to the peripheral pairs of microtubules in the axoneme. The flagellum also bears groups of long thin hairs, seen best in Figure 9A, but details of their point of attachment to the flagellar surface are not known.

The longitudinal flagellum: The longitudinal flagellum (Fig. 10A, B) lacks the hooks seen on the transverse flagellum. Internally, it contains ''packing material'' known from many other dinoflagellates (Fig. 10B). It also contains a striated fiber (Fig. 10A, B), a very unusual feature. Judging from Figure 10A,

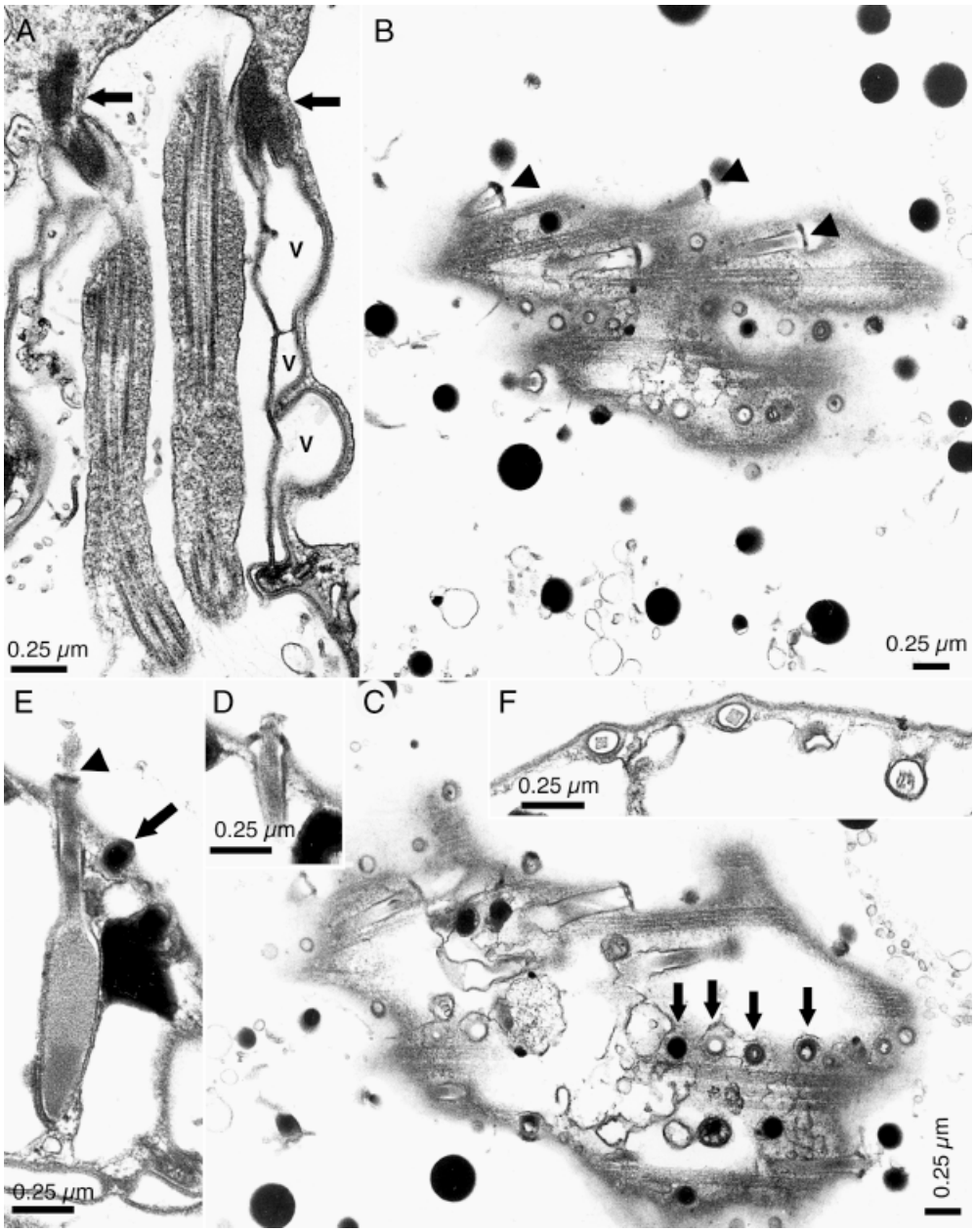

FIG. 7. The amphiesma of *Karlodinium armiger* sp. nov. (A) Longitudinal section through a pair of longitudinal flagella from a planozygote. The flagellar canal is covered with amphiesma vesicles (v), while such vesicles are absent outside the canal. The amphiesma vesicles appear empty. The arrows mark the collar of the flagellar canal. (B, C) Two consecutive sections from a series of tangential sections through the cell surface. The surface is bordered by numerous trichocysts (arrowheads), interspersed among bundles of microtubules, and rows of vacuoles with electron-opaque contents (arrows). Some of the latter are visible within the cell, but many have released their contents, which appear as opaque spheres around the cell. (D, E) Two consecutive sections through discharging trichocyst. The distal part of the trichocyst vesicle is covered with a lid-like structure (arrowhead in E), compare with (B). The arrow in (E) indicates one of the vacuoles with electron-opaque contents (see also B, C). (F) Section through the cell surface showing trichocyst necks (compare with the two trichocysts in Fig. 8A, C) and microtubules in oblique section.

the fiber appears to be involved in bending of the flagellum.

The pusule system: The pusule system is conspicuous (Fig. 11A–G). Two pusule systems appear to be present in the cell, one associated with each flagellar canal. Each pusule comprises a central tube (0.75–1 μm in diameter), lined by lateral tubes of smaller diameter (approximately 0.14 μm in diameter) and connected to the central tube through a slightly narrower aperture (Fig. 11F, G). The lumen side of each lateral tube is covered with a very thin layer of material, which is finely striated in two directions (Fig. 11E). The area between the lateral tubes is occupied by vacuoles, and a cross-section through a lateral tube therefore shows two concentric membranes (Fig. 11C). The innermost membrane represents the tube membrane; the outermost is the vacuole around the tube. Somewhat surprisingly, a membrane system appears to surround the entire system of lateral tubes (e.g., Fig. 11B, F, G). How this is related to the vacuoles around the tubes is not clear.

Pigment composition. Cells of *K. armiger* contain chl *a* and *c* (Fig. 12). The different types of chl *c* were not separated with the HPLC method used. The main carotenoid pigment is fucoxanthin, and additional carotenoids are 19′-hexanoyloxyfucoxanthin, diadinoxanthin, α- and β-carotene and three unidentified peaks with retention times of 14.6, 20.5, and 22.7 min, respectively. The retention time of 20.5 min

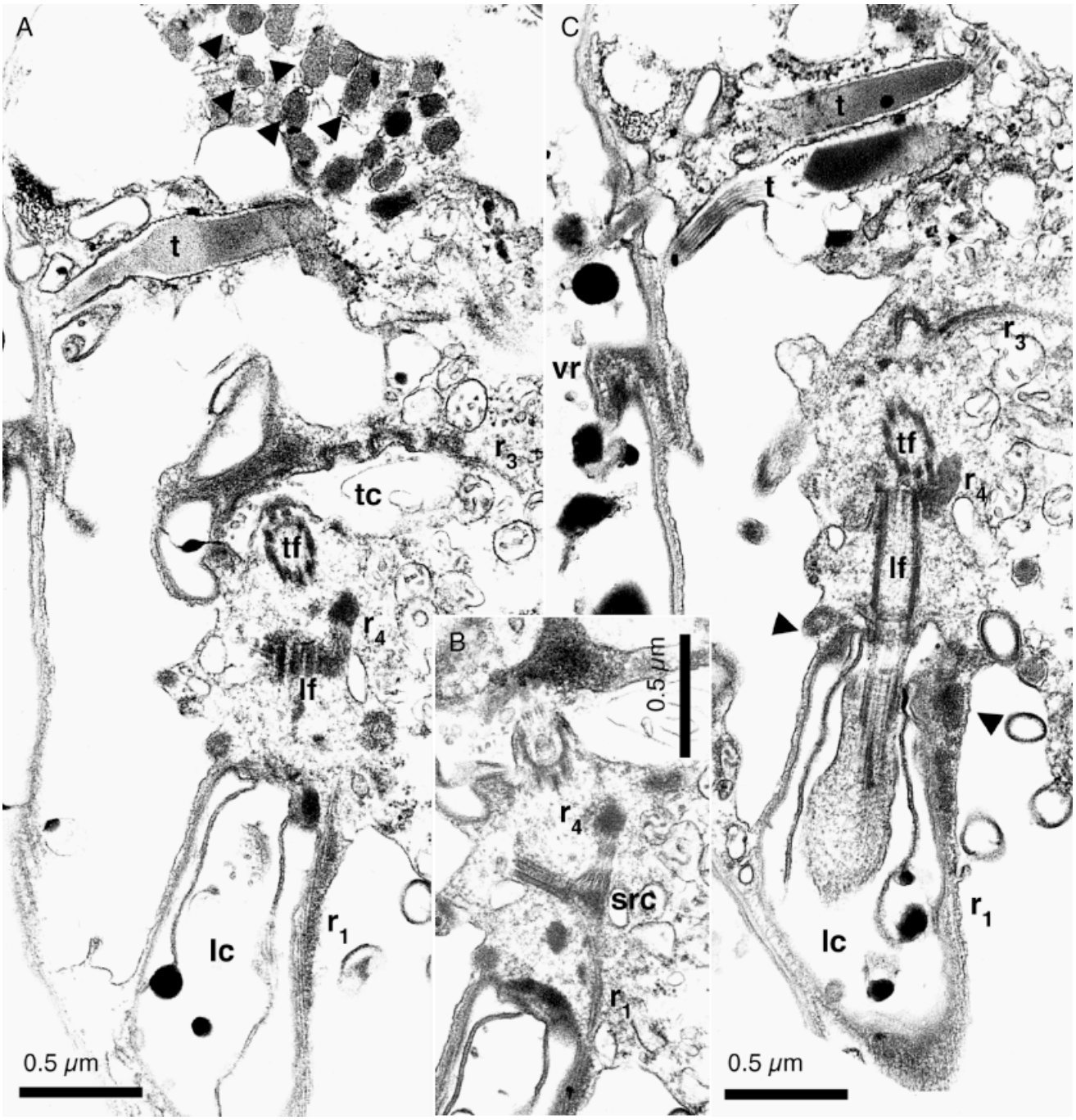

FIG. 8. Selected sections from a series of consecutive sections, showing features of the flagellar apparatus of *Karlodinium armiger* sp. nov. (A) Vacuoles of the peduncle (arrowheads), and the two flagellar bases (lf and tf) in the flagellar canals (lc and tc, respectively). Profiles of flagellar roots r_1 and r_4 are visible, together with the extension of r_3 which passes along the canal of the transverse flagellum; t, trichocyst. (B) Section immediately preceding (A), showing the striated fiber (src) that interconnects r_1 and r_4. (C) Two sections away from (A). The longitudinal flagellum has been sectioned precisely, and the collar around the canal of the longitudinal flagellum is visible. The arrowheads indicate the collar surrounding the longitudinal flagellar canal. Two trichocysts are present in the upper part of the micrograph (t), one in the process of discharging; vr, ventral ridge.

is identical to gyroxanthin-diester as described in Johnsen and Sakshaug (1993). The peak (22.7 min) is also similar to gyroxanthin-diester (Johnsen and Sakshaug 1993). Peridinin was not detected.

Toxicity by Artemia *tests.* Preliminary tests showed *K. armiger* to be toxic to *Artemia franciscana,* more so at 25° C than at 15° C. The results were somewhat inconsistent, however, probably because of the fact that cultures never became very dense, and will not be discussed further.

Karlodinium micrum (Leadbeater et Dodge) J. Larsen, strain K-0522

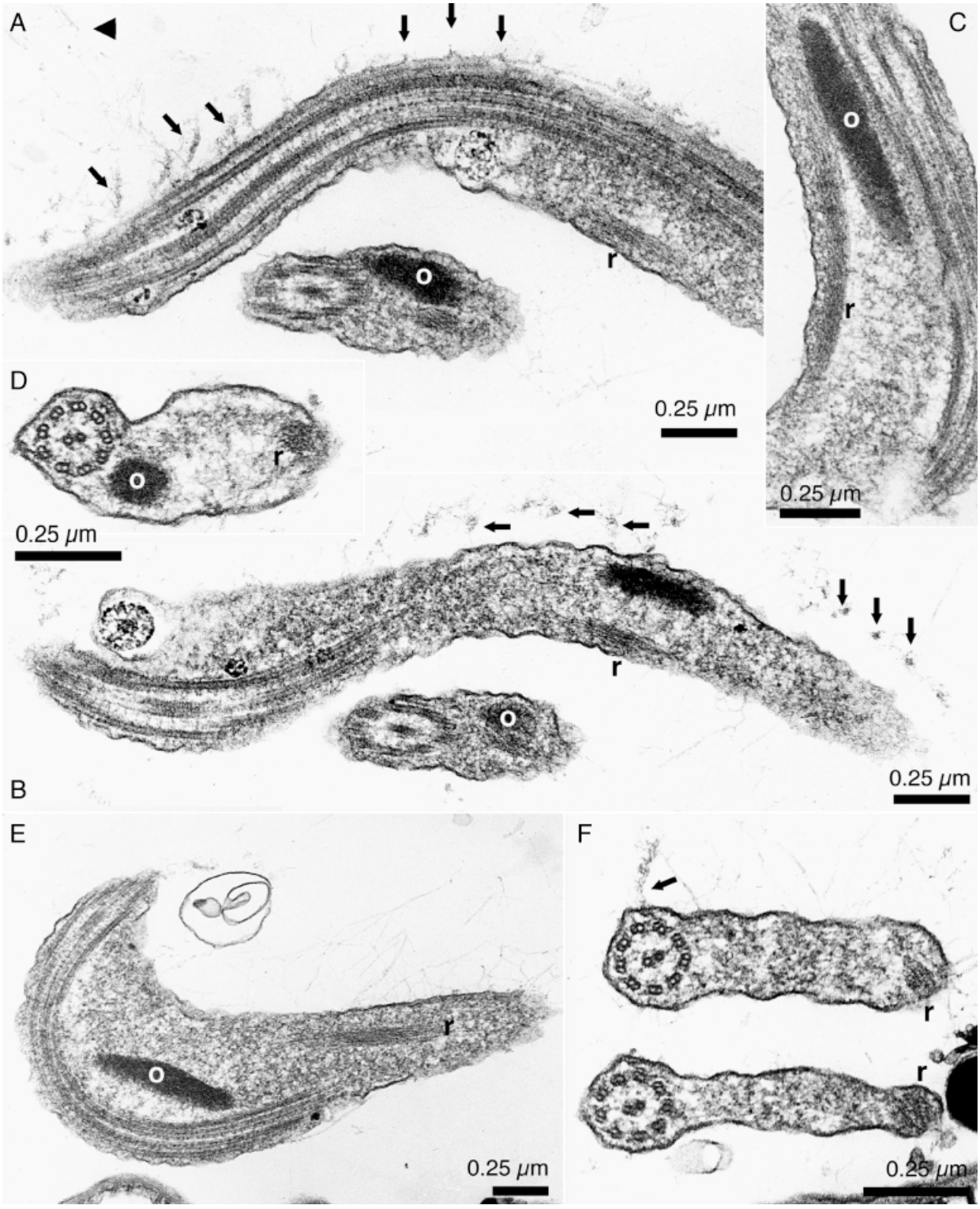

Fig. 9. Some details of the transverse flagellum in *Karlodinium armiger* sp. nov. (A, B) Two sections from a series through a pair of transverse flagella (from a planozygote), showing the supporting rod (r) and the opaque rod (o) in the flagellar wing. The unilateral row of hooks has been marked with arrows. A group of long thin hairs may perhaps be distinguished in (A) (arrowhead). (C) The supporting rod (r) is occasionally seen to be striated transversely; o, opaque rod. (D) Transverse section through transverse flagellum, illustrating both the supporting rod (r), located near the tip of the flagellar wing, and the opaque rod (o) near the axoneme. (E) From series of four sections, in which the opaque rod (o) was present in only the two middle sections, indicating that this structure if not continuous throughout the flagellum. (F) Transverse section through pair of transverse flagella (from planozygote), showing the flagellar wing. Each of the flagellar hooks (arrow) is probably attached through the flagellar membrane to doublets of the axoneme.

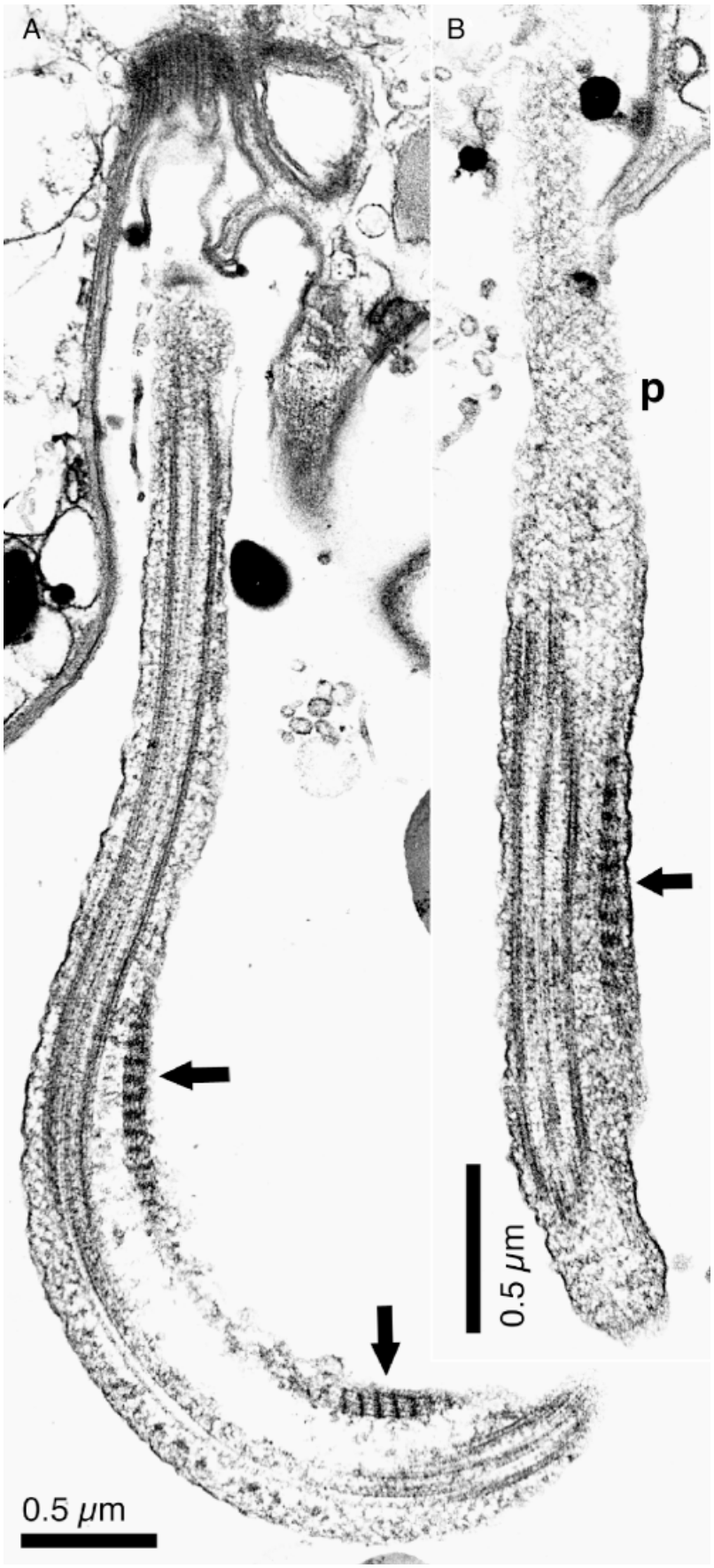

FIG. 10. (A, B) The longitudinal flagellum contains cross-banded "packing material" (p) as in many other dinoflagellates, and a very unusual muscle-like cross-banded fiber (arrows).

FIG. 11. Pusule system of *Karlodinium armiger* sp. nov. (A) Longitudinal section through a cell (planozygote), showing the position of the pusule systems in the cell (arrows). (B, D) Consecutive sections. The striated root (r_4) is very strongly developed and extends along a pusule canal, compare with (G); src the fiber that interconnects r_4 and r_1. (C) From the same series of sections, illustrating transverse sections of two lateral tubes of the pusule system. Each tube is surrounded by two membranes. (E) The lateral tubes are coated internally, giving the canal a striated appearance. (F) Section through the central canal of a pusule and associated lateral canals. The arrowheads indicate the membrane that surrounds the group of lateral canals, compare with (B), (C), and (G). (G) The central canal of a pusule in transverse section, showing lateral canals, two electron-opaque structures, representing the striated root r_4 (cf. 11B) and a group of microtubules on the right.

TABLE 2. Cell measurements and morphological characteristics of *Karlodinium armiger*, *K. veneficum* (K-0522 and Plymouth 103), and similar species.

	Karlodinium armiger	*Karlodinium veneficum* (K-0522) Syn. *K. micrum*)	*Karlodinium veneficum*[a] Plymouth 103	*Karlodinium vitiligo*[a]	*Gyrodinium corsicum*[b]	*Gyrodinium estuariale*[c]
Cell length (μm)	12–22 (17.4 ± 2.4, $n = 50$)	8–18 (13.6 ± 1.9, $n = 50$)	9–18	7–18	17–24	11–16
Cell width (μm)	8–18 (13.1 ± 1.8, $n = 50$)	8–14 11.1 ± 1.4, $n = 50$)	7–14	7–14	12–16	9–12
Length-to-width ratio	1.15–1.55 (1.33 ± 0.1, $n = 50$)	0.97–1.49 (1.23 ± 0.1, $n = 50$)	1.26[d]	1.21[d]	1.1[e]	1.3[e]
Girdle displacement %total cell length	29–36	23–32	<20 (from published figures)	<20 (from published figures)	32–34	<33
Sulcal extension	Yes	Yes	Yes	Yes	Yes	Yes
Apical groove	Straight, barely crossing apex, descending one-fourth down the dorsal epicone	Straight, descending one-seventh down the dorsal epicone	?	?	Descending one-third down the dorsal side, a curved base is directed to, but not connected to the sulcal extension	Apical region showing two concentric collar-like raised ridges, joining with the sulcal extension[f]
Ventral pore	Elongated pore (1 μm) to the left of the apical groove	Elongated pore (1 μm) to the left of the apical groove	?	?	Kidney-shaped pore, next to the curved base of the apical groove	?
Amphiesma structure	Granulated with numerous globular "dischargable" structures, randomly placed	Numerous minor depressions arranged in rows, every depression comprising a plug	Numerous minor depressions arranged in rows, every depression comprising a plug[g]	Numerous minor depressions arranged in rows, every depression comprising a plug[g]	Granulated, smoother on the hypocone, two parallel rows of pustular micro-processes on the hypocone	Vesiculated with thin plates[f]
Nucleus	Large, kidney-shaped, usually located in the left side of the hypocone	Large, round, located on the left side of the hypocone or centrally	Median, indistinct except prior to cell division	Median, indistinct except prior to cell division	Located centrally	Located centrally
Chloroplasts	Numerous (>10), elongate with lenticular pyrenoids, yellow-green in color	Two to four, with equal number in epi- and hypocone, orange-brown in color	Two to eight (usually four), irregular in shape, golden brown in color	Two to eight (usually four), irregular in shape golden brown in color	About 15 peripheral chloroplasts, green in color	Generally two, one in the epicone and one in the hypocone
Toxic	Yes	Yes	Yes	No	Possibly	Not detected

[a]Ballantine (1956).
[b]Paulmier et al. (1995).
[c]Hulburt (1957).
[d]Calculated on the basis of average figures.
[e]Assumed on the basis of the length and width.
[f]Gardiner et al. (1989).
[g]Dodge and Crawford (1970).

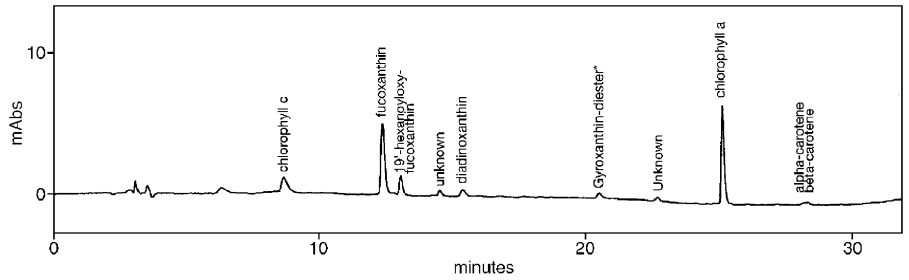

FIG. 12. Pigment profile of *Karlodinium armiger* sp. nov. *Absorption peaks corresponding to gyroxanthin-diester as described by Johnsen and Sakshaug (1993).

LM. Strain K-0522 is a small-to-medium-sized dinoflagellate with an average length of 13.6 ± 1.9 μm (range 8.1–17.5 μm) and an average width of 11.1 ± 1.4 μm (range 7.9–13.8 μm) ($n = 50$). See Table 2 for a comparison with *K. armiger*, *K. vitiligo*, *G. corsicum*, and *Gyrodinium estuariale*. The cell outline is oval and the epi- and hypocone are of about equal size. The epicone is conical or rounded, and the hypocone is rounded hemispherical (Fig. 13A, B). The cingulum is left-handed and excavated. It is displaced about two cingulum widths. Cingulum displacement is around one-third of the body length (Fig. 13A, B). The sulcus extends onto the epicone. The extension points upward to the right (Fig. 13A). The deep apical groove is seen as a minor cleft when focusing on the middle central plane (Fig. 13B). Each cell has two to four large chloroplasts, one to two in the epi- and one to two in the hypocone (Fig. 13B, D). They are golden-brown in color. The nucleus is large, round and situated in the left side of the hypocone or more centrally in the cell (Fig. 13C).

SEM. Ventrally, the apical groove begins just above the sulcal extension, in the mid-ventral plane (Fig. 14A). It extends in a rather straight line, past but not over the apex, onto the left dorsal side, and continues approximately one-seventh of the cell length, down the epicone. The groove is deep and about 0.5 μm wide along its entire length. The borders of the groove are distinctly thickened (Fig. 14A, C, D). A ventral pore is present to the left of the apical groove. It is elongate and approximately 1 μm long (Fig. 14A, E). The ventral ridge between the two flagellar pores possesses a distinct thickening (Fig. 14A). The angle between the sulcal extension and the ventral ridge is at least 90° and when viewed ventrally, this area appears as a soft curve (Fig. 14A, E). The outline of the lower right part of the epicone is conical (Fig. 14A). Several layers of membrane cover the cells. In some fixations, cells retained the outermost membrane and the amphiesma of polygonal vesicles (Fig. 14E). In others, the outer membrane of the vesicles was typically swollen with rounded blisters. They differed in size and shape, and some appeared to have collapsed, giving them a doughnut-like appearance (Fig. 14A). Whether the blisters are artifactual is unknown. Disappearance of the outer part of the amphiesma vesicles results in a species-characteristic structure of minor depressions arranged in rows (Fig. 14B, D), giving the cell a "goose-skin"-like appearance. When the outer part of the amphiesma vesicles is absent, trichocysts become visible, especially on the epicone (Fig. 14D). Each depression is believed to represent one of the plugs seen in TEM (Daugbjerg et al. 2000; Fig. 10). The amphiesma vesicles contain thin plates (Daugbjerg et al. 2000; Fig. 8).

TEM. We refer to Larsen's work in Daugbjerg et al. (2000).

Karlodinium veneficum (Ballantine) J. Larsen, culture Plymouth 103

Attempts to prepare the material for SEM were not successful. The fixation quality obtained for transmission electron microscopy was better, but preservation of certain cellular features, such as the cingulum, were not satisfactory. However, most details were well

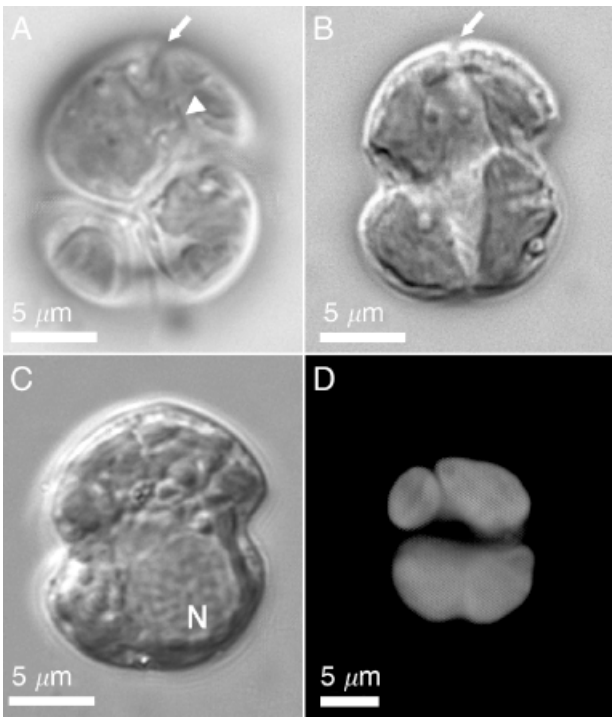

FIG. 13. Light and epifluorescence micrographs of *Karlodinium veneficum* (K-0522). (A) Cell in surface focus, showing the large chloroplasts, apical groove (arrow) and sulcal intrusion onto the epicone (arrowhead). (B) Cell in central focus showing the large chloroplasts and the apical groove (arrow). (C) Cell in central focus, showing the nucleus in the left side (N). (D) Cell showing the small number of autofluorescing large chloroplasts.

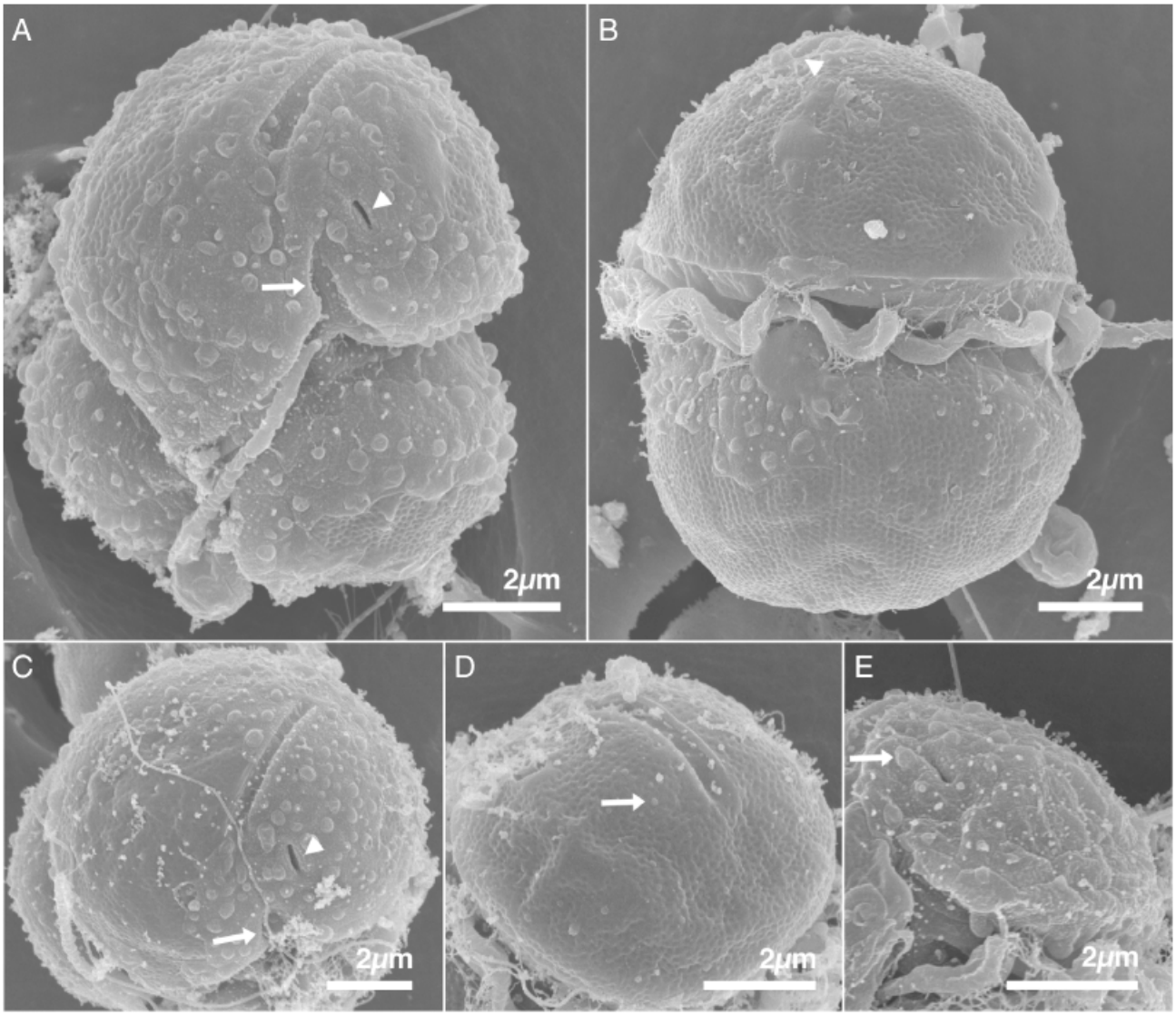

FIG. 14. Scanning electron micrographs of *Karlodinium veneficum* (K-0522). (A) Ventral view showing apical groove, ventral pore (arrowhead) and sulcal intrusion onto the epicone (arrow). (B) Dorsal view showing the longitudinal rows of depressions beneath the amphiesma vesicles, and the termination of the apical groove dorsally (arrowhead). (C) Apical view showing apical groove, ventral pore (arrowhead) and sulcal intrusion onto the epicone (arrow). (D) Dorsal apical view (arrow indicates trichocyst). (E) Ventral view of the left side of the epicone, showing the intact amphiesma vesicles. When the amphiesma vesicles are intact, they cover the minute depressions of the amphiesma that characterize this species; compare with (B) and (D). The white arrow indicates the ventral pore.

preserved, and selected features are shown in Figures 15–17. Two longitudinal sections through the cell at approximately right angles are shown in Figure 15A, B, which illustrate most of the organelles. The cell contained large vesicles beneath the amphiesma but their extended size may be a fixation artifact. The apical groove is visible in both figures. Figure 15C, D shows consecutive tangential sections through the cell, to illustrate the plug-like structures (arrows) located between the peripheral microtubules. The plugs may also be seen in a different orientation (at right angles), along the lowermost part of the cell in Figure 15B. Two consecutive sections through the ventral pore are illustrated in Figure 16A, B (a structure not illustrated in thin sections in any *Karlodinium* species so far), and show the pore to be covered throughout by amphiesmal cisternae. Within the cell, the pore is underlain by a flattened cisterna continuous with the larger vacuoles beneath the amphiesma. When preserved, the amphiesmal vesicles contain very thin material located next to the inner membrane (Fig. 16A, B).

The chloroplasts contain many pyrenoids of various shape (Fig. 16C). At higher magnification, their characteristic structure is readily visible; each pyrenoid being surrounded by a very thin opaque layer, which extends into a long beak. The pyrenoid matrix also commonly shows a tubular structure (not illustrated) as in Figure 6.

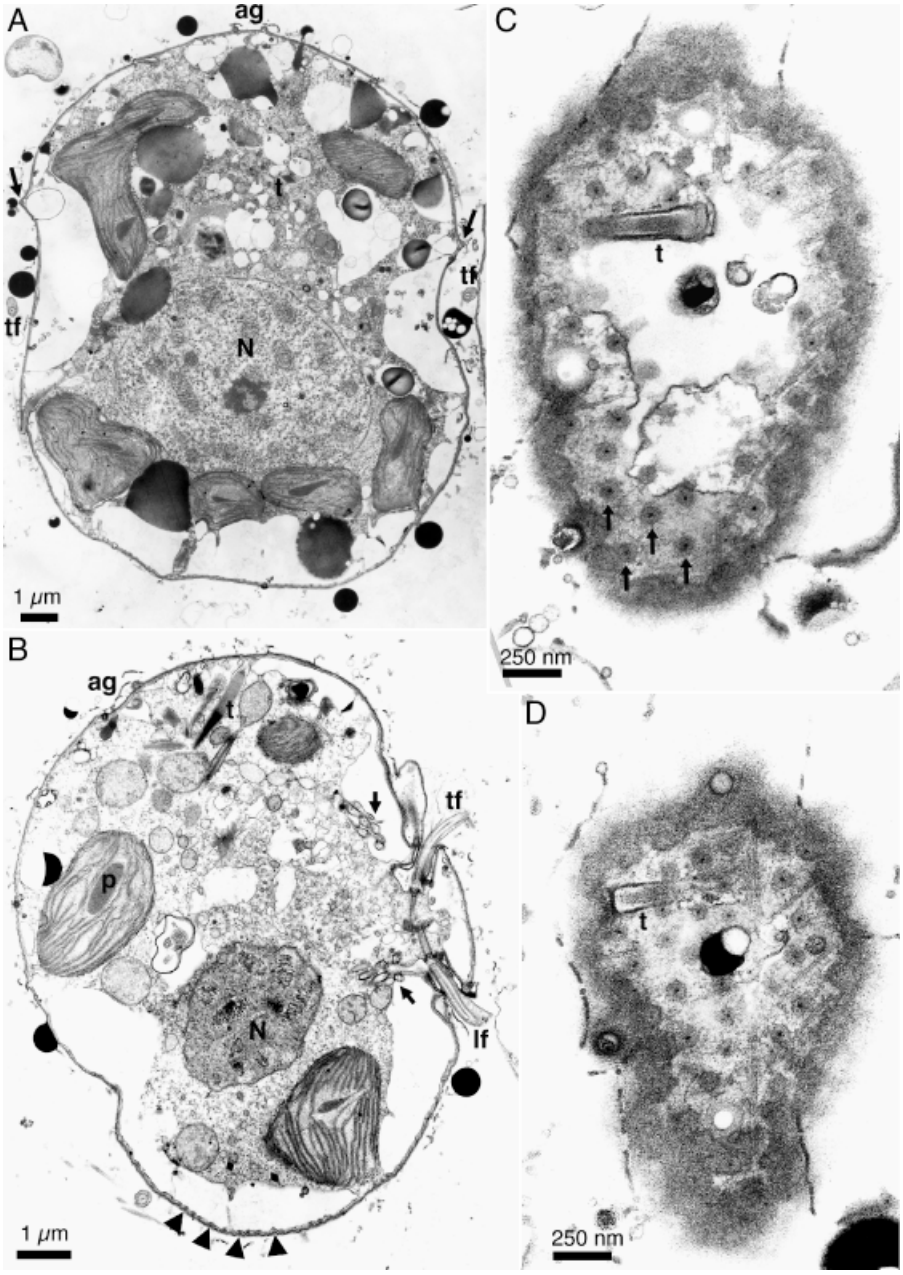

FIG. 15. *Karlodinium veneficum*, Culture 103, Plymouth Culture Collection. (A, B) Two longitudinal sections at almost right angles, illustrating the posterior nucleus (N), the peripheral chloroplasts, and the transverse flagellum (tf). The cingulum is marked anteriorly by a list (arrows in A) while the posterior part of the cingulum extends smoothly onto the hypocone. Ag is the apical groove; lf and tf the longitudinal and the transverse flagellum, respectively; *P* is a pyrenoid; *t* is a trichocyst; and the arrows in (B) mark the two pusule systems. The line of spheres along the posterior part of the cell exterior represent the plug-like structures (cf. C, D). (C, D) Consecutive, tangential sections through the cell surface, illustrating the plug-like structures (arrows) located between the cytoskeleton microtubules; t is a trichocyst vesicle.

The two flagella are inserted almost opposite, in two canals, each of which also shows the aperture of the two pusules visible in the cell (Fig. 17A, B). Figure 17B, and in particular Figure 17C (the three figures illustrate consecutive sections), also show the peduncle, the microtubules of which terminate between opaque material, and the peduncular collar (msc in Fig. 17C).

Molecular data and phylogenetic inference. Partial LSU rDNA sequences of the four *Karlodinium* isolates diverged 0.3%–7.7% (depending on method used to estimate the values) (Table 3). The sequence divergence between strains K-0522 (*K. micrum* in Daugbjerg et al. 2000) and *K. veneficum* (Plymouth 103) was only 0.3%, indicating that these are conspecific. A comparison of internal transcribed sequence (ITS) 1 and ITS 2 sequences of a strain identified as *K. micrum* from Chesapeake Bay (USA) and *K. veneficum* (Plymouth 103) further confirmed that *K. micrum* and *K. veneficum* are conspecific (Daugbjerg, unpublished). While using the same DNA fragment, the divergence between species of *Karlodinium* is similar to that of closely related species of *Karenia* (2.2%–9.4%) and *Takayama* (2%–4%) (data not shown).

The three species of *Karlodinium* included formed a monophyletic genus in phylogenetic analyses based on ML, MP, and NJ (Fig. 18). However, the genus only received high bootstrap support for its monophyletic

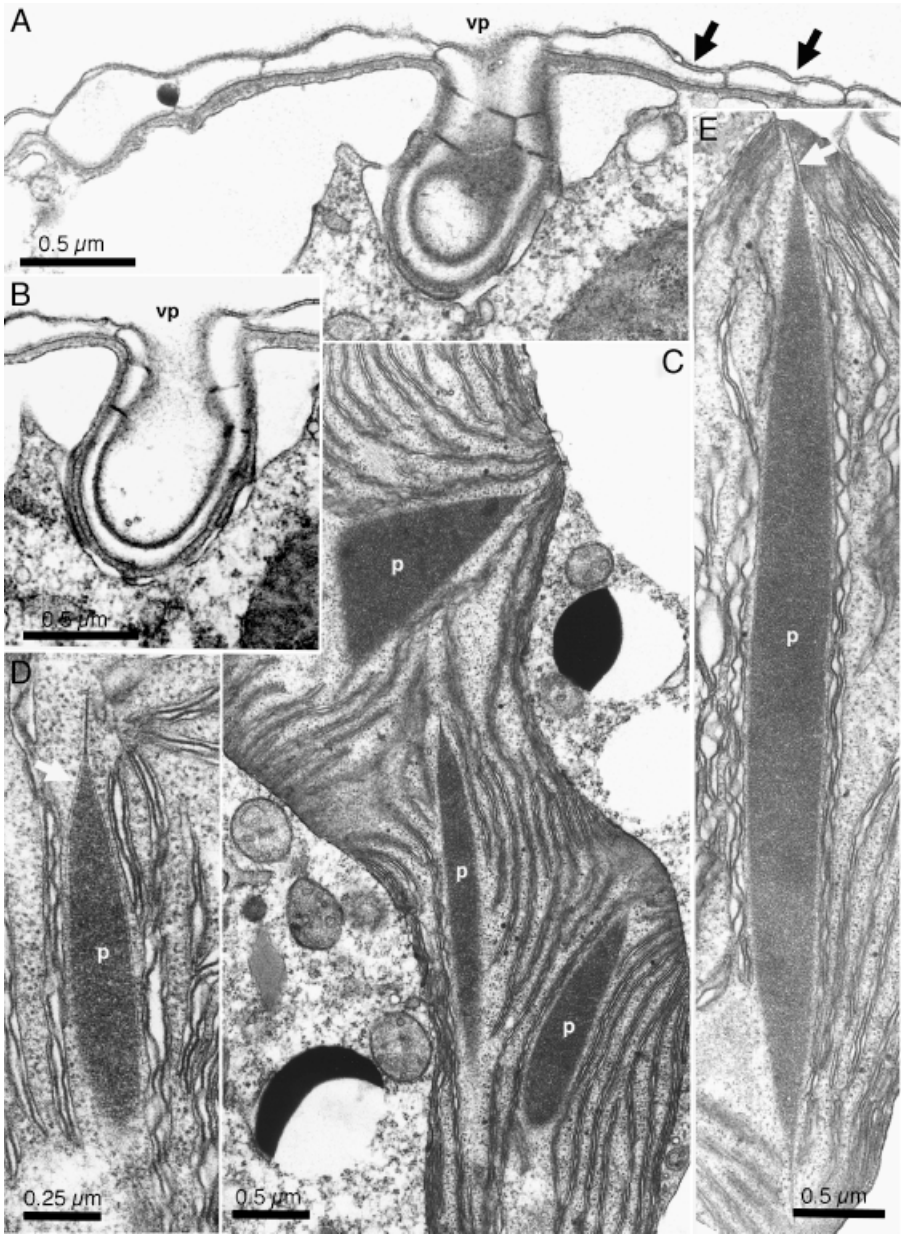

FIG. 16. *Karlodinium veneficum*, Plymouth Culture 103. (A, B) Two consecutive sections through the ventral pore (vp), which externally is covered by amphiesmal cisternae and internally by a flattened vesicle. Two amphiesmal cisterna have been marked by arrows in A. (C, D, E) The chloroplasts contain many pyrenoids (p), each of which is lined by a thin opaque layer (white arrow in D) that extends into a beak or wing (white arrow in E).

status in ML and MP analyses. The branching order revealed *K. veneficum* as sister taxon to *K. armiger* and *K. australe*, with moderate to well-supported bootstrap values. *Karlodinium* was the sister to *Takayama,* and the two genera formed the sister group to *Karenia*. The order of branching is similar to that described by de Salas et al. (2003). However, support for the topology of some of the *Karenia* species was low as revealed by the very short branch lengths, especially for the deep branches in the *Karenia* lineage, including *K. papilionacea* and *K. bidigitata* (Fig. 18).

DISCUSSION

Karlodinium veneficum *versus* K. micrum. The type species of *Karlodinium, K. micrum,* is morphologically very similar to *K. veneficum* (Ballantine 1956) (Table 2; Fig. 19). This applies to both LM, SEM, and TEM. In our TEM of *K. veneficum,* we found the plugs that characterize *K. micrum*, and all other details were also identical. As mentioned above, the estimated LSU rDNA sequence divergence between strains identified as *K. micrum* (the original strain from England has been lost) and the strain Plymouth 103, the culture on which the description of *K. veneficum* was based in 1956, was only 0.3% (Table 3). This is similar to values for isolates of *Karenia mikimotoi* (sequence divergence = 0.2%; Hansen et al. 2000) and for two isolates of *K. umbella* from separate locations in Tasmania (sequence divergence = 0.1%). Hence, the sequence divergence between populations from different geographic areas is less than 0.5% when

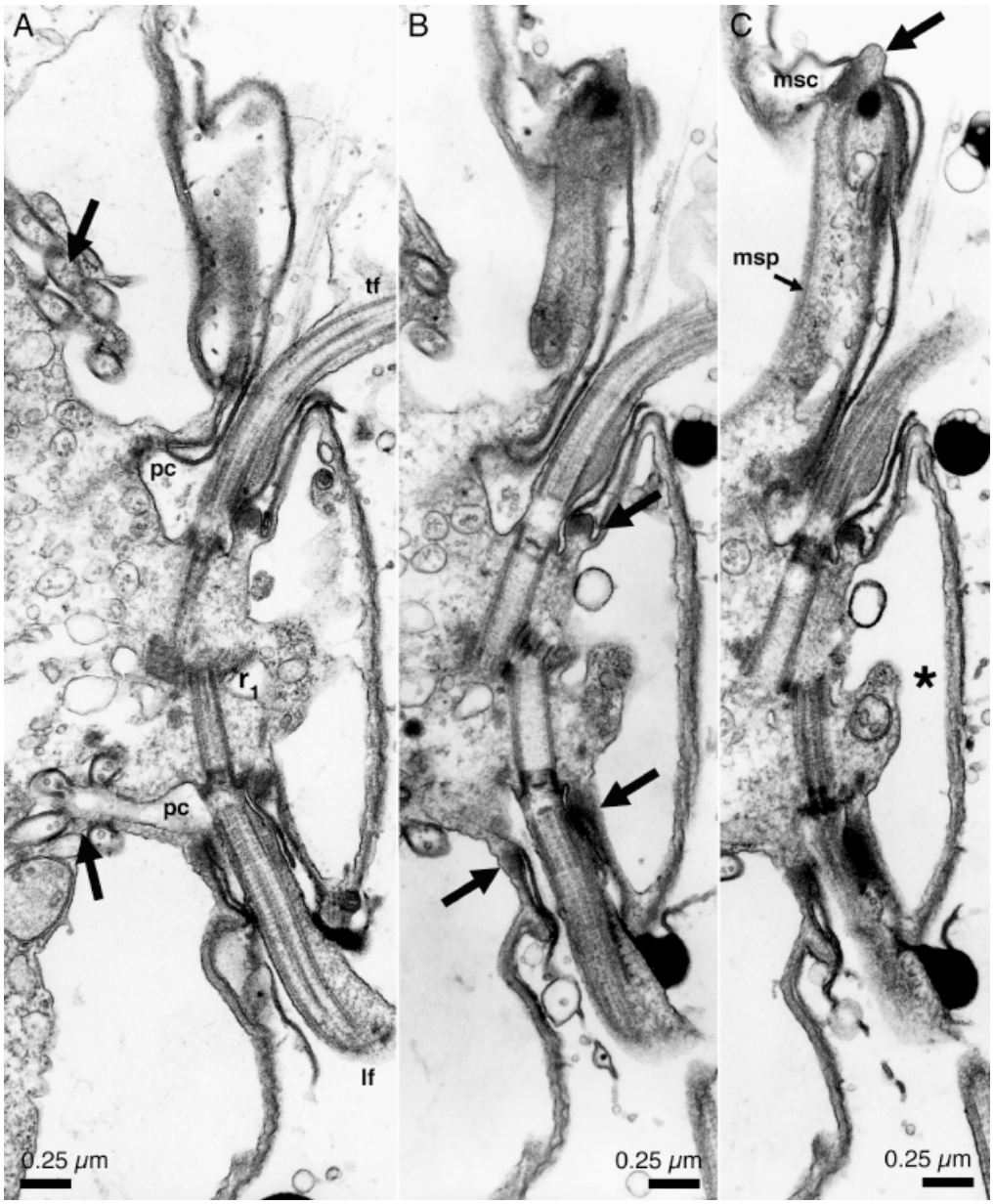

FIG 17. *Karlodinium veneficum*, Plymouth Culture 103. The two flagella (lf and tf) are inserted almost oppositely to each other, each flagellum emerging through a flagellar canal surrounded proximally by an opaque collar (arrows in B). The two pusule canals (pc) interconnect the pusule systems (one marked by arrow in A) with the two flagellar canals; msp is the microtubular strand of the peduncle, and msc is the collar that surrounds the msp near the cell surface (arrow). The asterisk indicates the ventral flap containing the ventral ridge. One of the flagellar roots is visible next to the longitudinal flagellar base in A (r_1).

based on this fragment of the LSU rDNA gene. For species belonging to the *Karenia–Karlodinium–Takayama* lineage, sequence divergences based on this gene fragment appears to be 2%–9%. In cell size, *K. micrum* and *K. veneficum* are identical. *K. veneficum* cells are 9–18 μm long ($\bar{x} = 12$ μm) and 8–14 μm wide ($\bar{x} = 10$ μm) according to Ballantine (1956). *K. micrum* cells range between 8 and 18 μm in length ($\bar{x} \pm \text{SD} = 13.6 \pm 1.9$ μm) and between 8 and 14 μm in width ($\bar{x} \pm \text{SD} = 11.1 \pm 1.4$ μm). The two taxa therefore overlap in length-to-width ratio (Table 2). *K. veneficum* was described with equally sized epi- and hypocone, the epicone being more pointed (Ballantine 1956). The drawing of *K. veneficum* shows a cell with a slightly pointed epicone (Fig. 19B, C), which we have seen also in *K. micrum* (Fig. 13C). We have also observed cells of *K. micrum* with a more broadly rounded epicone (Fig. 13A, B). Ballantine (1956) described *K. veneficum* as possessing two to eight chloroplasts, typically with two chloroplasts in the epi- and two in the hypocone. The color was described as golden-brown. The same holds for our observations on *K. micrum*. A sulcal extension and a centrally located nucleus were described in *K. veneficum* (Ballantine 1956), which also correlates with *K. micrum*. Neither the presence of an apical groove nor the structure of the amphiesma was described by Ballantine (1956), but Dodge and Crawford (1970) provided information about the structure of the amphiesma, which appeared to be similar to that of *K.*

TABLE 3. Sequence divergence (in percentage) between species of *Karlodinium* based on 1438 bp of large subunit (LSU) rDNA gene.

	K. armiger (K-0668)	*K. veneficum* (K-0522)	*K. veneficum* (Plymouth no. 103)	*K. australe*
Karlodinium armiger (K-0668)	—	4.8	4.5	4.4
Karlodinium veneficum (K-0522)	4.9	—	0.3	7.3
Karlodinium veneficum (Plymouth no. 103)	4.6	0.3	—	6.9
Karlodinium australe	4.5	7.7	7.3	—

Strain numbers are provided in parentheses. Estimates of sequence divergences are based on uncorrected ("p") (above diagonal) and Kimura 2-parameter (below diagonal) using PAUP*.

micrum. This particular type of amphiesma has not been observed in any other species of *Karlodinium*. When first examined by EM (as *Woloszynskia micra*, Plymouth culture 207) by Leadbeater and Dodge (1967a), each chloroplast was said to be bounded by a double membrane. The following year, the existence of three bounding chloroplast membranes in the majority of dinoflagellates was detected (Dodge 1968), but the number of membranes in *Karlodinium* is actually difficult to ascertain. In our fixations, the impression was that only two membranes are present, but this feature needs to be examined using a range of fixatives before a conclusion about the number of membranes can be made. None of the published illustrations of chloroplasts in *K. micrum* show the number of membranes clearly (e.g., Leadbeater 1971; Fig. 12, bottom left).

It is not possible to distinguish between the two taxa *K. veneficum* and *K. micrum* morphologically, and considering the very small difference in partial LSU, we conclude that the two species are conspecific. This finding leads to a name change for the type species of *Karlodinium* to *K. veneficum*, and reduces the name *K. micrum* to a synonym.

Synopsis. ***Karlodinium veneficum*** (Ballantine) J. Larsen

Basionym: G. veneficum Ballantine (1956}, P. 469

Taxonomic synonyms: K. micrum (Leadbeater et Dodge) J. Larsen in Daugbjerg et al. (2000), *G. galatheanum* Braarud *sensu* Kite and Dodge (1988), and their nomenclatural synonyms: *Gymnodinium micrum* (Leadbeater et Dodge) Loeblich III, *Gyrodinium galatheanum* (Braarud) Taylor, *W. micra* Leadbeater et Dodge (1966).

Type locality: Hamoaze, over Rubble Bank, off King William Point, South Yard, Devonport, England.

Distribution: K. micrum has been reported from the North Sea; British Isles; Oslo Fjord, Norway; Whangakoko, South Island, New Zealand; Swan River, Perth, Western Australia; St. Johns River, Florida, USA; Neuse River, North Carolina, USA; Maryland, USA: Princess Anne Co., Manokin River, Hyrock fish farm, Chesapeake Bay; South Atlantic Ocean: Walvis Bay, South Africa (data from GenBank: http://www.ncbi.nlm.nih.gov/). Owing to the similarity between the different species of *Karlodinium,* the reports need to be confirmed.

The other species of Karlodinium. *K. veneficum* and *K. armiger* are well separated both morphologically and in partial LSU rDNA sequences. The differences have been assembled in Table 2, which also contains data from the literature on *K. vitiligo*, *G. corsicum,* and *G. estuariale*.

K. armiger differs from *K. veneficum* in the shape of the right ventral part of the epicone (pointed in *K. armiger*, more rounded in *K. veneficum*), the length of the apical groove on the dorsal side of the cell, and in amphiesma structure (Table 2). In SEM and TEM, cells of *K. armiger* are seen to lack the minor depressions or plugs arranged in rows in a hexagonal configuration in *K. veneficum* (Leadbeater and Dodge 1966). Leadbeater and Dodge (1966) described *K. micrum* (as *W. micra*) with two chloroplasts, one in the epicone and one in the hypocone. Our material of *K. veneficum* (Fig. 12D) usually contained four chloroplasts, two in the epicone and two in the hypocone. The color of the chloroplasts was described by Leadbeater and Dodge (1966) as yellow-green, while in our material, the color was golden-brown. *K. armiger* has numerous (>10) small chloroplasts, which are elongated or droplet shaped, and pale yellow-green in color. The nucleus is situated in the left side of the hypocone in both *K. armiger* and *K. veneficum* (Figs. 2B and 13C, respectively). The photosynthetic pigments of *K. armiger*, notably the possession of fucoxanthin, 19′-hexanoyloxyfucoxanthin, gyroxanthin-diester and the absence of peridinin resemble the pigment composition of *K. veneficum* (Johnsen and Sakshaug 1993). The two adjacent peaks of gyroxanthin-diester found in *K. veneficum* (Chesapeake Bay-isolate and Hilton Head pond isolate) (Kempton et al. 2002), agree with our findings in *K. armiger*. *K. veneficum* also possesses the pigment 19′-butanoyloxyfucoxanthin, which was not detected in *K. armiger*.

Ultrastructurally, the two species *K. armiger* and *K. veneficum* share many features, and they are closely related. Features shared between the two species are the detailed construction of the apical groove, the construction of the cingulum (with an anterior list but smooth posteriorly), the type of pyrenoid, the flagellar insertion, etc.

Gyrodinium corsicum Paulmier, Berland, Billard et Nezan is closely related and undoubtedly a member of *Karlodinium*. Its cells contain about 15 green chloroplasts, and each cell bears two rows of minute processes on the hypocone (Paulmier et al. 1995). We have never seen such processes in *K. armiger*. The nucleus in *G. corsicum* is centrally located (Paulmier et al. 1995).

Gyrodinium estuariale Hulburt resembles *K. armiger* in size, shape and girdle displacement, but it possesses two to four golden-brown chloroplasts as in *K. veneficum* (Table 2; Fig. 19). Hulburt (1957) in the original

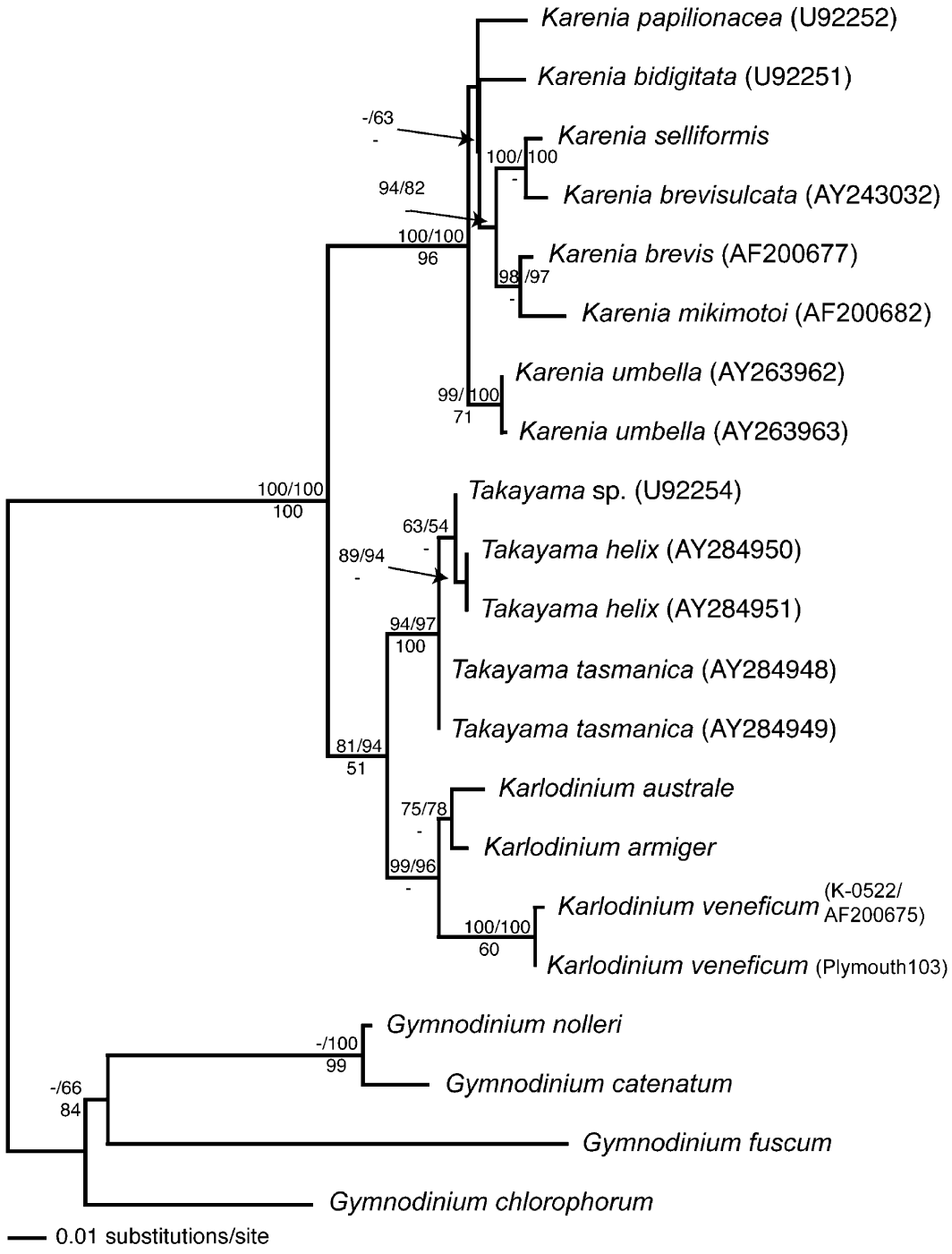

FIG. 18. Phylogeny of the *Karenia–Karlodinium–Takayama* lineage of dinoflagellates inferred from partial large subunit rDNA sequences (1367 bp of which 239 were parsimony informative), based on neighbor-joining (NJ) using maximum likelihood (ML) parameters as suggested by Modeltest. In ML analyses, the best ln likelihood score was—4883.165, using the TrN + I + G model with settings as suggested by Modeltest. Maximum parsimony (MP) analyses resulted in nine equally parsimonious trees, each of 589 steps (CI = 0.767, RI = 0.854). Bootstrap values $\geq$50% are shown to the left of internal nodes. The first numbers are from ML analyses (100 replications), the second numbers are from MP analyses (10,000 replications) and the last numbers are from NJ analyses (1000 replications). Four species of *Gymnodinium* were used to root the tree. The branch lengths are proportional to the number of substitutions per site. *Takayama* and *Karlodinium* are sister groups, and together they constitute the sister group to *Karenia*.

description did not mention an apical groove but Gardiner et al. (1989) provided electron micrographs of material from Tampa Bay, Florida, identified as *G. estuariale*. There is some confusion, however, as the SEMs included in the article show a thecate dinoflagellate with an apical pore complex as in *Pfiesteria* or *Scrippsiella*. The TEM shows cells with very delicate plates in the amphiesma vesicles, and chloroplasts with

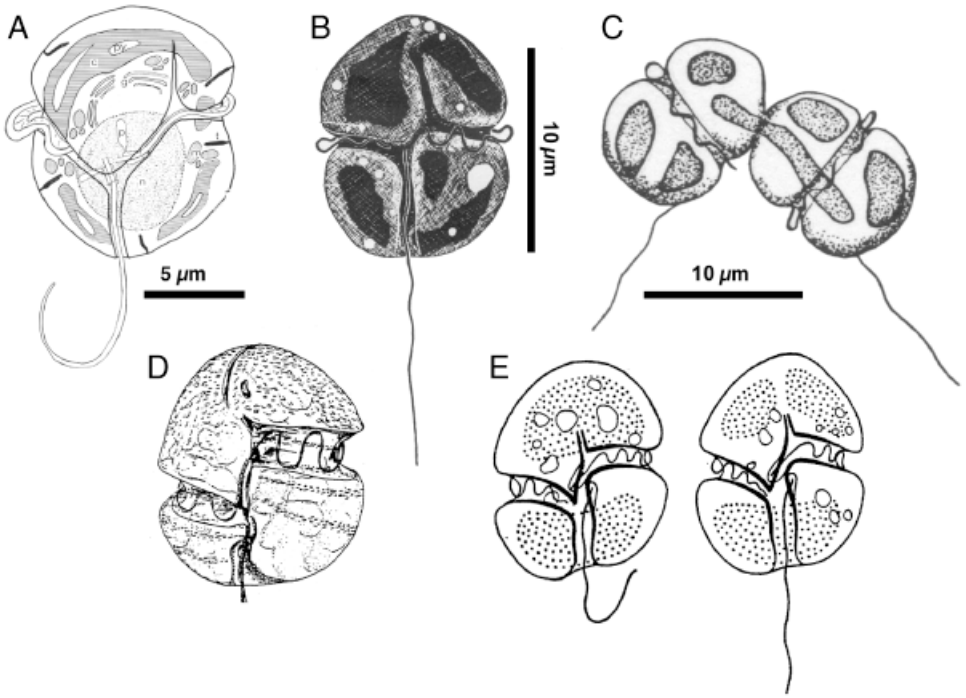

FIG. 19. Members of the *Karlodinium* group. (A). *Woloszynskia micra* (from Leadbeater and Dodge 1966). (B, C). *Gymnodinium veneficum* (from Ballantine 1956). (D). *Gyrodinium corsicum* (from Paulmier et al. 1995). (E). *Gyrodinium estuariale* (from Hulburt 1957).

lenticular pyrenoids (Gardiner et al. 1989). The amphiesma resembles that of *K. armiger*. Hulburt (1957) noted that *Gymnodinium estuariale* resembled *K. veneficum*, but differed in a greater girdle displacement, a wider, deeper girdle and sulcus, and the oblique instead of symmetrically rounded antapex. Further examination of *G. estuariale* is needed to establish whether this species is also a synonym of *K. veneficum*.

Gymnodinium galatheanum Braarud from Namibia was described in a very incomplete way by Braarud (1957), based on formaldehyde-preserved material. Its taxonomic fate remains unresolved. An isolate isolated recently from Namibia and believed to be conspecific with *G. galatheanum* may not belong to this species. Rather it may be *Gymnodinium aureolum* or a related species (Velikova et al. 2004). Braarud (1957) drew *G. galatheanum* with a central apical notch, indicating that it belongs in *Karlodinium* or *Karenia*. *Karlodinium vitiligo* (Ballantine) J. Larsen differs in minor details from *K. veneficum*, and the two species may be conspecific (Table 2).

Sexual reproduction in Karlodinium. A full understanding of the sexual reproduction in *K. armiger* is lacking, but we have often observed two cells attached to each other and swimming in circles. The point of attachment was the apex, possibly the apical groove, or the central part of the ventral side, possibly the ventral ridge (inset in Fig. 4). The gamete fusion resembles that reported in *K. brevis*, a closely related species (Walker 1982). The presence of two parallel sets of flagella and flagellar roots in many cells also prove them to be planozygotes (von Stosch 1973). In Leadbeater and Dodge (1967a), Figures 13 and 18 illustrate planozygotes of *K. veneficum* (as *W. micra*) and some of Ballantine's (1956) drawings of *G. veneficum,* interpreted by her as division stages, may represent stages in cell fusion (Ballantine, 1956, illustrations on *P.* 473 and shown here as Fig. 19C). In Leadbeater and Dodge (1967b), claimed to show nuclear and cell division in *K. veneficum* (as *W. micra*), Figures 1–3 clearly show planozygotes, not dividing cells, and the process described as mitosis may perhaps be meiosis in the planozygote. We did not observe hypnocysts or temporary cysts, indicating that *K. armiger* lacks a cyst stage. In the closely related *Karenia mikimotoi* (Miyake et Kominami *ex* Oda) Gert Hansen & Moestrup, hypnocysts have never been seen either despite many studies. Planozygotes were very common in our cultures, indicating that the planozygote stage is long-lasting, a feature seen also in certain other dinoflagellates: two weeks in *Alexandrium tamarense* and *Lingulodinium polyedrum* (Anderson et al. 1983, Figueroa and Bravo 2005) and up to four weeks in a form of *Peridinium bipes* F. Stein (Park and Hayashi 1992). Probably the planozygote in *Karlodinium* divides without producing a hypnozygote.

Food uptake in Karlodinium. Material examined by Li et al. (1996, as *G. galatheanum*) was shown to be mixotrophic and Li et al. (1999) illustrated a short peduncle. Our TEM sections have shown the presence of a peduncle also in *K. armiger* and *K. veneficum*. We are presently examining food uptake and the food uptake process in *K. armiger.*

Toxicity. K. veneficum is known to be toxic to a variety of animals (Abbott and Ballantine 1957, Deeds et al. 2002). One or more toxins, named karlotoxins (KmTx1 and KmTx2), have been isolated from

strains of *K. veneficum* (as *K. micrum*) (Bachvaroff and Place 2004). The toxins are polyhydroxy-polyenes that increase ionic permeability of membranes to a range of small ions and molecules, and kill fish by damaging gill epithelia (Deeds et al. 2002, Deeds and Place 2004, Place 2004). The toxic effect described by Abbott and Ballantine (1957) in *K. veneficum* resembles that found recently in isolates from the USA, named *K. micrum*, supporting the notion that the two taxa are conspecific (Deeds, personal communication).

Emendation of the genus Karlodinium. As mentioned above, *K. armiger* lacks the plug-like structures that infer a hexagonal appearance to the amphiesma of K. *veneficum*. To date, this structure has been detected only in *K. veneficum*. However, the definition of Karlodinium J. Larsen (Daugbjerg et al. 2000) excludes species with a different amphiesma structure. Because all other morphological, molecular and pigment data support the inclusion of *K. armiger* in *Karlodinium*, the description of the genus *Karlodinium* needs to be emended.

Karlodinium J. Larsen (emended): Unarmored dinoflagellates with chloroplasts containing internal, lenticular pyrenoids and fucoxanthin or fucoxanthin derivatives as main accessory pigments; apical groove straight; ventral pore present.

Karlodinium is closely related to *Karenia*, the main known morphological difference being the ventral pore in *Karlodinium*. A structure shared between *K. armiger* and *K. veneficum* is the presence of unilateral hooks on the transverse flagellum. This unusual feature is presently known only in species of *Karlodinium* (Leadbeater and Dodge 1966) and in the heterotrophic species *Gyrodinium lebouriae* Herdman (Lee 1977). The latter does not belong in *Gyrodinium sensu* Gert Hansen and Moestrup, but its phylogeny is unknown. A somewhat similar structure is known in the perkinsid *Parvilucifera* (Norén et al. 1999), which is only distantly related to *Karlodinium*. The presence of hooks should be searched for in *Karenia* and *Takayama*. Is this character shared between all three genera (a synapomorphy), or is it a character of *Karlodinium* only? The longitudinal flagellum of *K. armiger* is unusual in its possession of a conspicuous striated fiber. This structure is almost certainly present also in *K. veneficum* (Leadbeater and Dodge 1967a, as *W. micra*), and we agree with Hansen (2001) that Leadbeater and Dodge confused the transverse and longitudinal flagellum in their sections (loc.cit. Figs. 13–15). *Ceratium* also possesses fibers used in retraction of the longitudinal flagellum (Maruyama 1982) but they are very different from that of *Karlodinium*. Surprisingly, a striated fiber of *K. armiger* type occurs in *Gymnodinium aureolum* (Hansen 2001).

A separate evolutionary lineage. The genera *Takayama*, *Karenia*, and *Karlodinium* are closely related, and this is reflected in the morphology and in the photosynthetic pigment profile. A major difference between *Takayama* on one hand, and *Karenia* and *Karlodinium* on the other, is the shape of the apical groove: sigmoid in *Takayama* and straight in *Karenia* and *Karlodinium*. In the phylogenetic tree, *Takayama* and *Karlodinium* appear to be more closely related to each other than *Karenia* and *Karlodinium* (Fig. 18), but this is not supported by the outline of the apical groove.

We propose a new family for the evolutionary lineage comprising *Karenia*, *Karlodinium*, and *Takayama*:

Kareniaceae fam. nov.

Dinoflagellata inermia, quorum chloroplasti fucoxanthinum aut de fucoxanthino oriunda habent. Sulcus apicalis rectus aut s-formis.

Unarmoured dinoflagellates whose chloroplasts contain fucoxanthin or fucoxanthin-derivatives. Apical groove straight or s-shaped.

In Copenhagen, Charlotte Hansen is thanked for technical help running the sequences on the ABI 377, and Lisbeth Haukrogh for help with sectioning for TEM. We thank Miguel de Salas for allowing us to include his LSU rDNA sequence of *K. australe* sp. nov. before publication, and Gert Hansen for providing a culture of *K. selliformis* from Tunesia. Peter Henriksen kindly did the pigment analysis. We also thank Anders Friis for preparing Fig. 3. N. D. thanks the Carlsberg Foundation for equipment grants. In Plymouth, Ø. M. thanks John Green and Mariata Jutson at the Marine Biological Association for assistance, and Roy M. Moate at Plymouth Electron Microscopy Centre, University of Plymouth for permission to use his laboratory for preparation of Plymouth 103 for electron microscopy and DNA sequencing. Finally, we thank Jonathan Deeds for unpublished information on the karlotoxins. This study was supported by the Danish Science Research Council (project no. 21–02–0539).

Abbott, B. C. & Ballantine, D. 1957. The toxin of *Gymnodinium veneficum* Ballantine. *J. Marine Biol. Assoc. UK* 36:169–89.

Anderson, D. M., Chisholm, S. & Watras, C. 1983. Importance of life cycle events in the population dynamics of *Gonyaulax tamarensisr. Marine Biol.* 76:179–89.

Bachvaroff, T. R. & Place, A. R. 2004. Distinguishing strains of Karlodinium micrum based on microsatellite markers. Abstracts from XI International Conference on Harmful Algal Blooms, Cape Town, November 14–19, 2004, p. 63.

Ballantine, D. 1956. Two new marine species of *Gymnodinium* isolated from the Plymouth area. *J. Marine Biol. Assoc. UK* 35:467–74.

Braarud, T. 1957. A red water organism from Walvis Bay (*Gymnodinium galatheanum* n. sp.). *Galathea Rep.* 1:137–8.

Daugbjerg, N., Moestrup, Ø. & Arctander, P. 1994. Phylogeny of the genus *Pyramimonas* (Prasinophyceae, Chlorophyta) inferred from the *rbc*L gene. *J. Phycol.* 30:991–9.

Daugbjerg, N., Hansen, G., Larsen, J. & Moestrup, Ø. 2000. Phylogeny of some of the major genera of dinoflagellates based on ultrastructure and partial LSU rDNA sequence data, including the erection of three new genera of unarmoured dinoflagellates. *Phycologia* 39:302–17.

Deeds, J. R., Terlizzi, D. E., Adolf, J. E., Stoecker, D. K. & Place, A. R. 2002. Toxic activity from cultures of *Karlodinium micrum* (= *Gyrodinium galatheanum*)(Dinophyceae)—a dinoflagellate associated with fish mortalities in an estuarine aquaculture facility. *Harmful Algae* 1:169–89.

Deeds, J. R. & Place, A. R. 2004. *Sterol specific membrane interactions with the toxins from Karlodinium micrum (Dinophyceae)—a strategy for self-protection*. Abstracts from XI International Conference on Harmful Algal Blooms, Cape Town, November 14–19, 2004, p. 98.

Delgado, M. 1998. *Report of the monitoring of toxic phytoplankton in Catalonia*, No. 1. CSIC and DARP, Barcelona.

Delgado, M. & Alcatraz, M. 1999. Interactions between red tide microalgae and herbivorous zooplankton: the noxious effects of *Gyrodinium corsicum* (Dinophyceae) on *Acartia grani* (Copepoda: Calanoidea). *J. Plankton Res.* 21:2361–71.

de Rijk, P., Wuyts, J., van de Peer, Y., Winkelmanns, T. & de Wachter, R 2000. The european large subunit ribosomal RNA database. *Nucl. Acids Res.* 28:177–83.

de Salas, M. F., Bolch, C. J. S., Botes, L., Nash, G., Wright, S. W. & Hallegraeff, G. M. 2003. *Takayama* gen. nov. (Gymnodiniales, Dinophyceae), a new genus of unarmoured dinoflagellates with sigmoid apical grooves, including the description of two new species. *J. Phycol.* 39:1233–46.

Dodge, J. D. 1968. The fine structure of chloroplasts and pyrenoids in some marine dinoflagellates. *J. Cell Sci.* 3:41–8.

Dodge, J. D. & Crawford, R. M. 1970. A survey of thecal fine structure in the Dinophyceae. *Bot. J. Linn. Soc.* 63:53–67.

Figueroa, R. I. & Bravo, I. 2005. Sexual reproduction and two different encystment strategies of *Lingulodinium polyedrum* (Dinophyceae) in culture. *J. Phycol.* 41:370–9.

Fraga, S. & Moestrup, Ø. 2004. Dinoflagellates—Order Gymnodiniales. In IOC Taxonomic Reference List of Toxic Algae (Ed. Ø. Moestrup). Intergovernmental Commission of UNESCO. http://www.ioc.unesco.org/hab/data/htm.

Gardiner, W. E., Rushing, A. E. & Dawes, C. J. 1989. Ultrastructural observations of *Gyrodinium estuariale* (Dinophyceae). *J. Phycol.* 25:178–83.

Hansen, G. 2001. Ultrastructure of *Gymnodinium aureolum* (Dinophyceae): toward a further redefinition of *Gymnodinium sensu stricto*. *J. Phycol.* 37:612–23.

Hansen, G., Daugbjerg, N. & Henriksen, P. 2000. Comparative study of *Gymnodinium mikimotoi* and *Gymnodinium aureolum*, comb. nov. (= *Gyrodinium aureolum*) based on morphology, pigment composition, and molecular data. *J. Phycol.* 36: 394–410.

Hulburt, E. M. 1957. The taxonomy of unarmoured Dinophyceae of shallow embayments on Cape Cod, Massachusetts. *Biol. Bull.* 112:196–219.

Johnsen, G. & Sakshaug, E. 1993. Bio-optical characteristics and photoadaptive responses in the toxic and bloom-forming dinoflagellates *Gyrodinium aureolum*, *Gymnodinium galatheanum*, and two strains of *Prorocentrum minimum*. *J. Phycol.* 29: 627–42.

Kempton, J. W., Lewitus, A. J., Deeds, J. R., Law, J. M. & Place, A. R. 2002. Toxicity of *Karlodinium micrum* (Dinophyceae) associated with a fish kill in a South Carolina brackish retention pond. *Harmful Algae* 1:233–41.

Kite, G. C. & Dodge, J. D. 1988. Cell and chloroplast ultrastructure in *Gyrodinium aureolum* and *Gymnodinium galatheanum*. Two marine dinoflagellates containing an unusual carotenoid. *Sarsia* 73:131–8.

Leadbeater, B. S. C. 1971. The intracellular origin of flagellar hairs in the dinoflagellate *Woloszynskia micra* Leadbeater & Dodge. *J. Cell Sci.* 9:443–51.

Leadbeater, B. S. C. & Dodge, J. D. 1966. The fine structure of *Woloszynskia micra* sp. nov., a new marine dinoflagellate. *Br. Phycol. Bull.* 3:1–17.

Leadbeater, B. S. C. & Dodge, J. D. 1967a. An electron microscope study of dinoflagellate flagella. *J. Gen. Microbiol.* 46:305–14.

Leadbeater, B. S. C. & Dodge, J. D. 1967b. An electron microscope study of nuclear and cell division in a dinoflagellate. *Arch. Mikrobiol.* 57:239–54.

Lee, R. E. 1977. Saprophytic and phagocytic isolates of the colourless heterotrophic dinoflagellate *Gyrodinium lebouriae* Herdman. *J. Marine Biol. Assoc. UK* 57:303–15.

Li, A., Stoecker, D. K., Coats, D. W. & Adam, E. J. 1996. Ingestion of fluorescently-labeled and phycoerythrin-containing prey by photosynthetic dinoflagellates. *Aquat. Microb. Ecol.* 10:139–47.

Li, A., Stoecker, D. K. & Adolf, J. E. 1999. Feeding, pigmentation, photosynthesis and growth of the mixotrophic dinoflagellate *Gyrodinium galatheanum*. *Aquat. Microb. Ecol.* 19:163–76.

Maruyama, T. 1982. Fine structure of the longitudinal flagellum in *Ceratium tripos*, a marine dinoflagellate. *J. Cell Sci.* 58:109–23.

Norén, F., Moestrup, Ø. & Rehnstam-Holm, A. S. 1999. *Parvilucifera infectans* Norén et Moestrup gen. et sp. nov. (Perkinsozoa phylum nov.): a parasitic flagellate capable of killing toxic microalgae. *Eur. J. Protistol.* 35:233–54.

Park, H. D. & Hayashi, H. 1992. Life cycle of *Peridinium bipes* f. *occultatum* (Dinophyceae) isolated from Lake Kizaki. *J. Fac. Sci. Shinshu Univ.* 27:87–104.

Paulmier, G., Berland, B., Billard, C. & Nezan, E. 1995. *Gyrodinium corsicum* nov. sp. (Gymnodiniales, Dinophycées), organisme responsible d'une "eau verte" dans l'etang marin de Diana (Corse), en avril 1994. *Cryptogamie Algol.* 16:77–94.

Place, A. 2004. *Amphidinols and karlotoxins—brothers in arms*. Abstracts from XI International Conference on Harmful Algal Blooms, Cape Town, November 14–19, 2004, p. 211.

Posada, D. & Crandall, K. A. 1998. Modeltest: testing the model of DNA substitution. *Bioinform. Applic. Note* 14:817–18.

Schlüter, L. & Havskum, H. 1997. Phytoplankton pigments in relation to carbon contents of phytoplankton communities. *Marine Ecol. Prog. Ser.* 15:55–65.

Swofford, D. L. 2003. *PAUP* Phylogenetic Analysis Using Parsimony (* and Other Methods), Version 4.0b.10*. Sinauer Associates, Sunderland, MA.

Tamura, K. & Nei, M. 1993. Estimation of the number of nucleotide substitutions in the control region of mitochondrial DNA in humans and chimpanzees. *Mol. Biol. Evol.* 10:512–26.

Velikova, V., Louw, D., Pienaar, R. & Sym, S. 2004. *Dinoflagellates in the benguela current waters off namibia*. Abstracts from XI International Conference on Harmful Algal Blooms, Cape Town, November 14–19, 2004, p. 252.

von Stosch, H. A. 1973. Observations on vegetative reproduction and sexual life cycles of two freshwater dinoflagellates, *Gymnodinium pseudopalustre* Schiller and *Woloszynskia apiculata* sp. nov. *Br. Phycol. J.* 8:105–34.

Walker, L. M. 1982. Evidence for a sexual cycle in the Florida red tide dinoflagellate, *Ptychodiscus brevis* (= *Gymnodinium breve*). *Trans. Am. Microsc. Soc.* 101:287–93.